

Eukaryotic translation initiation factor 2 α kinase 2 in pancreatic cancer: An approach towards managing clinical prognosis and molecular immunological characterization

HAO-XUAN DU¹, HU WANG¹, XIAO-PENG MA¹, HAO CHEN¹, AI-BIN DAI¹ and KE-XIANG ZHU¹⁻³

¹The First Clinical Medical College, Lanzhou University; ²Department of General Surgery;

³Key Laboratory of Biotherapy and Regenerative Medicine of Gansu Province, The First Hospital of Lanzhou University, Lanzhou, Gansu 730000, P.R. China

Received February 20, 2023; Accepted July 14, 2023

DOI: 10.3892/ol.2023.14066

Abstract. Most patients with pancreatic cancer are already in the late stages of the disease when they are diagnosed, and pancreatic cancer is a deadly disease with a poor prognosis. With the advancement of research, immunotherapy has become a new focus in the treatment of tumors. To the best of our knowledge, there is currently no reliable diagnostic or prognostic marker for pancreatic cancer; therefore, the present study investigated the potential of eukaryotic translation initiation factor 2 α kinase 2 (EIF2AK2) as a predictive and diagnostic marker for pancreatic cancer. Immunohistochemical staining of clinical samples independently verified that EIF2AK2 expression was significantly higher in clinically operated pancreatic cancer tissues than in adjacent pancreatic tissues, and EIF2AK2 expression and differentially expressed genes (DEGs) were identified using downloadable RNA sequencing data from The Cancer Genome Atlas and Genomic Tumor Expression Atlas. In addition, Gene Ontology/Kyoto Encyclopedia of Genes and Genomes analyses and immune cell infiltration were used for functional enrichment analysis of EIF2AK2-associated DEGs. The clinical importance of EIF2AK2 was also determined using Kaplan-Meier survival, Cox regression and time-dependent survival receiver operating characteristic curve analyses, and a predictive nomogram model was generated. Finally, the functional role of EIF2AK2 was assessed in PANC-1 cells using a short hairpin RNA-EIF2AK2 knockdown approach, including CCK-8, wound healing assay, cell cycle and apoptosis assays. The findings suggested that EIF2AK2 may have

potential as a diagnostic and prognostic biomarker for patients with pancreatic cancer. Furthermore, EIF2AK2 may provide a new therapeutic target for patients with pancreatic cancer.

Introduction

Pancreatic cancer is a particularly deadly type of gastrointestinal malignancy. Due to the difficulty of early diagnosis and the limited effectiveness of treatment with surgery, radiotherapy and chemotherapy, patients with pancreatic cancer have a poor prognosis and high mortality rate, with an overall survival rate of only 8% at 5 years (1). Ductal adenocarcinoma of the pancreas is the most common type, accounting for 95% of all cases of pancreatic cancer (2). Most patients with pancreatic cancer are diagnosed at an advanced stage, so only 15-20% of patients with pancreatic cancer can undergo surgery. In addition, pancreatic cancer has a high rate of recurrence even after radical resection (3). Studies have shown that the malignant progression, treatment resistance and poor prognosis of pancreatic cancer are significantly linked to the immunosuppressive nature of the tumor microenvironment (TME) of pancreatic cancer (4-6). Although immunotherapy has achieved significant results in tumors, such as breast, lung and ovarian cancer, immunotherapy has not been effective in pancreatic cancer due to the highly suppressive nature of the tumor immune microenvironment (7,8). Therefore, it is crucial to research the immunological microenvironment of pancreatic cancer. By focusing on its constituents and inhibitory characteristics, researchers are expected to provide new ideas and directions for immunotherapy of pancreatic cancer.

Over 10 cell types have been reported to routinely express eukaryotic translation initiation factor 2 α kinase 2 (EIF2AK2) and it may be activated by a variety of cellular stresses, such as viral infections, hypoxia and nutritional shortages (9,10). The significance of EIF2AK2 in cancer remains controversial and complex. In general, EIF2AK2 is considered to have tumor suppressive functions (11-14). Several studies have demonstrated a link between EIF2AK2 suppression or inactivation and poor prognosis in a variety of malignancies, including breast, lung and colorectal cancer (15,16). Invasive ductal carcinoma cells have been shown to express higher levels of

Correspondence to: Professor Ke-Xiang Zhu, Department of General Surgery, The First Hospital of Lanzhou University, 1 Donggang West Road, Chengguan, Lanzhou, Gansu 730000, P.R. China
E-mail: flexzhu6910@sina.com

Key words: eukaryotic translation initiation factor 2 α kinase 2, pancreatic cancer, prognosis, immune infiltrates, tumor microenvironment

EIF2AK2 compared with normal breast tissue (17). In addition, the expression and activity levels of EIF2AK2 are linked to the probability of breast cancer cells spreading (18). The activation of EIF2AK2 by double-stranded RNA (dsRNA) has also been documented to be involved in the management of breast cancer cell mobility (19). These results indicated that EIF2AK2 may have a crucial role in suppressing cancer metastasis. However, EIF2AK2 has also been reported to be associated with the proliferation and migration of hepatocellular carcinoma, and the metastasis of gastric cancer (20,21). Therefore, it is possible that its antitumor or oncogenic function of EIF2AK2 depends on the type of cancer cells. Notably, to the best of our knowledge, the relationship between EIF2AK2 expression and pancreatic cancer, and its predictive value, has not been investigated.

The present study aimed to investigate the relationship between EIF2AK2 expression and survival outcomes in patients with pancreatic cancer using The Cancer Genome Atlas (TCGA), Genomic Tumor Expression Atlas (GTEx) and Gene Expression Omnibus (GEO) datasets. The present study examined whether there is a correlation between EIF2AK2 mRNA levels and the presence of immune cells in tumors. The results of the present study highlight the potential importance of EIF2AK2 in pancreatic cancer and shed light on the methods by which EIF2AK2 may interact with the tumor immune system.

Materials and methods

EIF2AK2 gene expression analysis. UCSC XENA (<https://xenabrowser.net/datapages/>) Functional Genome Browser, with 1098 public datasets from 91 cohorts including TCGA, ICGC, TARGET, GTEx and CCLE, is a next-generation online data analysis and visualization platform that integrates analysis, visualization, and Galaxy. Therefore, the pancancer analysis and the prognostic outcome relied on RNA sequencing data from TCGA (dataset no. TCGA-PAAD.htseq_fpkm.tsv; 178 human PAAD tumors and 4 non-malignant pancreas samples) and the GTEx (dataset no. gtex_gene_expected_count, 167 non-malignant pancreas samples) databases, both of which were available from UCSC XENA (22-24). Additionally, EIF2AK2 expression data from normal and tumor tissues were obtained from GEO datasets (<https://www.ncbi.nlm.nih.gov/geo/>) (25,26): GSE15471 (pairs of normal and tumor tissue samples were obtained at the time of surgery from resected pancreas of 36 pancreatic cancer patients) (27), GSE16515 (this consists of 36 tumor samples and 16 normal samples; a total of 52 samples; 16 samples consist of both tumor and normal expression data, whereas 20 samples consist of only tumor data) (28), GSE32676 (42 human PDAC tumors and 7 non-malignant pancreas samples snap-frozen at the time of surgery were chosen) (29) and GSE62165 (118 human PDAC tumors and 13 non-malignant pancreas samples snap-frozen at the time of surgery were chosen) (30), in order to assess their expression differences. UALCAN online analysis software (<http://ualcan.path.uab.edu/index.html>) was additionally employed to examine EIF2AK2 protein levels. Ultimately, the protein expression levels of EIF2AK2 in tumors and normal tissues were verified using The Human Protein Atlas database (THPA; <https://www.proteinatlas.org/>).

Cells and reagents. The hTERT-HPNE, MIA PaCa-2, PANC-1, AsPC-1 and SW1990 cell lines were purchased from The Cell Bank of Type Culture Collection of The Chinese Academy of Sciences. E.Z.N.A. Total RNA Kit I kit was purchased from Omega Bio-Tek Co., Ltd. (cat. no.: R6834-01). Evo M-MLV Reverse Transcription Premix Kit (cat. no. AG11728), SYBR Green Pro Taq HS Premix qPCR Kit (cat. no. AG11701) and ROX Reference Dye (cat. no. AG11703) were purchased from Accurate Biology Co., Ltd. LV-EIF2AK2-RNAi Lentivirus and the corresponding RNAi-negative lentivirus were purchased from Shanghai GeneChem Co., Ltd. (cat. no. GIEL0368481. The generation system was a second generation self-inactivating lentiviral packaging system and the supplier of the interim cell line used (293T cells) was Shanghai GeneChem, Co., Ltd. The GV quantity of lentiviral plasmid was vector Plasmid: 20 μ g, pHelper 1.0 vector plasmid: 15 μ g, pHelper 2.0 vector plasmid: 10 μ g). Anti-EIF2AK2 (1:1,000; cat. no. 18244-1-AP; Proteintech Group, Inc.), anti-AKT (1:1,000; cat. no. BS-2720R; BIOSS), anti-phosphorylated (p)-AKT (1:1,000; cat. no. GTX121937; GeneTex, Inc.) and anti-GAPDH (1:1,000; cat. no. ab128915; Abcam) were used in the present study. The 5X protein loading buffer, electrophoresis solution and Tris-Glycine Transfer Buffer were purchased from Wuhan Servicebio Technology Co., Ltd. The PVDF membrane was purchased from Millipore Sigma.

Cell culture and infection. Human normal pancreatic cell lines (hTERT-HPNE) and human pancreatic cancer cell lines (MIA PaCa-2, PANC-1 and SW1990) were cultured in DMEM (cat. no. SH30243.01; Cytiva) with 10% fetal bovine serum (cat. no. AB-FBS-0500; ABW) and the AsPC-1 pancreatic cancer cell line was cultured with 1640 medium (Cytiva; cat. no. SH30809.01) containing 10% fetal bovine serum. All cell lines were grown in a 37°C and 5% CO₂ constant-temperature incubator. The cells were digested with trypsin and 2 ml complete medium was aspirated and mixed to make a single-cell suspension. Then, 200-300 μ l single-cell suspension was added to a 6-well cell culture plate and the medium was replenished to 2 ml. The 6-well cell culture plate was removed from the constant-temperature incubator on alternate days, and the cell status and density were observed under an inverted microscope.

Lentiviral infections were performed when the cell confluence was 70%. The virus was infected with the cells at a concentration of 3.0x10⁹ TU/ml, and the lentiviral transfection reagent HiTrans G P/A was also added in 25 μ l of each reagent. After 12h, fluorescence expression was observed under a biological inverted microscope (RCX41; Ningbo Sunny Precision Industry Co., Ltd). When the cell density reached 90%, 4 ml of DMEM medium containing 2 μ g/ml (PANC-1; MOI=2) puromycin was added, and the culture continued to be incubated at 37°C for 24 h. After 48 h of incubation, the expression of the green fluorescent protein was then observed under a fluorescence microscope to ensure a stable infection. By using RT-quantitative PCR (RT-qPCR), highly efficient transfected cells were obtained for further experiments. The primers used for the assay were as follows: EIF2AK2 forward, 5'-GGCATT CAGCTCCACACTTG-3' and reverse, 5'-ACAGACGAGTGA TACCAGCG-3'; GAPDH forward, 5'-AGGGCTGCTTTT AACTCTGGT-3' and reverse, 5'-CCCCACTTGATTTTG

GAGGGA-3'; EIF2AK2-RNAi (115396-2): 5'-GAAGGTGAA GGTAGATCAAAG-3'; EIF2AK2-RNAi (115397-1): 5'-GGA ATTACATAGGCCTTATCA-3'; EIF2AK2-RNAi (115398-1): 5'-GACAGTTTAAACAGTTCTTCG-3'; RNAi-negative control: 5'-TTCTCCGAACGTGTACGT-3'.

RT-qPCR. RT-qPCR was used to examine the mRNA expression levels of EIF2AK2 in pancreatic cell lines and to assess knockdown efficiency after infection of PANC-1 cells for 48 h. Total RNA was extracted from cells with E.Z.N.A. Total RNA Kit I and cDNA was synthesized according to the Evo M-MLV Reverse Transcription Premixed Kit. qPCR was performed to amplify the cDNA using the Evo M-MLV Reverse Transcription Premix Kit with the primers listed in Table SI. The following thermocycling conditions were used: Stage 1, 95°C for 30 sec; Stage 2, 95°C for 5 sec and 60°C for 30 sec, 40 cycles; Stage 3 (dissociation curve), 95°C for 15 sec, 60°C for 1 min and 95°C for 15 sec. Relative gene expression was calculated using the $2^{-\Delta\Delta C_q}$ method (31) and GAPDH was used as the control gene.

Western blotting. Cells were lysed by radioprecipitation with lysis buffer containing RIPA lysate (cat. no. G2002; Wuhan Servicebio Technology Co., Ltd.) and 1% phenylmethylsulfonyl fluoride (MilliporeSigma) for 30 min at 4°C. The total protein lysate was then collected and the concentration determined using a BCA protein assay kit (cat. no. PC0020; Wuhan Servicebio Technology Co., Ltd.). Subsequently, denatured proteins (30 μ g/lane) were separated on a 12% SDS-PAGE gel and transferred to a PVDF membrane (cat. no. IRVH00010; MilliporeSigma). After being blocked with 5% skimmed milk (cat. no. D8340, Solarbio) for 1.5 h at room temperature, the membranes were incubated with EIF2AK2 primary antibody, AKT and p-AKT overnight at 4°C, followed by goat anti-rabbit (dilution 1:3,000; cat. no. RS0002; ImmunoWay Biotechnology Company) secondary antibody conjugated to horseradish peroxidase for 1 h at room temperature. The densities of the specific protein bands were visualized and captured using Image J (National Institutes of Health, v.1.8.0).

Clinical sample collection. A total of 48 paraffin-embedded tumor tissue samples and 48 paraffin-embedded adjacent tissues collected between September 2020 and August 2022 were obtained from The First Hospital of Lanzhou University (Gansu, China). The clinicopathological data of 48 patients with pancreatic cancer from the First Hospital of Lanzhou University were extracted, which showed a total of 23 males (47.9%) and 25 females (52.1%), with a mean age of 62 years and an age range of 37-83 years. All patients had a postoperative pathological diagnosis of pancreatic ductal cell carcinoma, and none received chemotherapy or radiation therapy. All patients provided written informed consent and the present study was approved by the Ethics Committee of the First Hospital of Lanzhou University (approval no. LDY YLL2023-304).

Immunohistochemical staining. Pathological specimens (paraffin-embedded sections on glass slides) were collected, and underwent dewaxing, hydration (dewaxing and hydration of paraffin sections: Xylene I and II for 25 min each, different gradients of ethanol 100, 95, 90, 85, 80, 70% for

10 min each) and antigen retrieval (sodium citrate at 95°C twice for 5 min each, followed by 3 washes with PBS for 5 min each). Subsequently, 3% hydrogen peroxide was incubated for 15 min followed by dropwise closure with normal goat serum and incubation at 37°C for 30 min. The sections were incubated with EIF2AK2 primary antibody (1:100, cat. no. 18244-1-AP; Proteintech Group, Inc.) overnight at 4°C. Then the sections were incubated with the EIF2AK2 secondary antibody (1:100, cat. no. 18244-1-AP; Proteintech Group, Inc.) at 37°C for 30 min, followed by the addition of a tertiary antibody (horseradish peroxidase labelled streptavidin working solution, cat. no. SP-9001; Broad Spectrum.) and incubation at 37°C for 30 min. DAB (1:20) color development was carried out for 8 min and observed under the microscope. Hematoxylin re-staining was carried out at room temperature for 60 sec, followed by gradient alcohol dehydration (70% for 5 min, 80% for 5 min, 85% for 5 min, 90% for 5 min, 95% for 10 min, and 100% for 10 min). Finally, the slices were cleared with xylene (xylene I and II for 25 min each) before being sealed with neutral resin. The results were observed and analyzed: Three fields were randomly selected under the fluorescence microscope (Leica DM2500; Leica Microsystems GmbH) and the images were analyzed by Image-Pro Plus software (Media Cybernetics, Inc. v.6.0). SP Kit (Broad Spectrum, cat. no. SP-9001) and DAB Substrate kit (cat. no. ZLI-9018) were purchased from OriGene Technologies, Inc. Hematoxylin (cat. no. G1080), neutral gum (cat. no. G8590) and 0.01 M sodium citrate buffer (cat. no. C1010) were purchased from Beijing Solarbio Science & Technology Co., Ltd.

Cell Counting Kit-8 (CCK-8) assay. After trypsin digestion of the cells, 100 μ l (~ 2×10^3 cells/100 μ l) cell suspension was added to each well of a 96-well plate. The plates were incubated in a 37°C incubator for 3-4 h until the cells were fully attached to the plates. After incubation at 37°C for 12, 24, 48 and 72 h, 10 μ l of CCK-8 solution (cat. no. CA1210; Beijing Solarbio Science & Technology Co., Ltd.) was added to each well and incubated for a further 3 h. Absorbance at 450 nm was measured with a spectrophotometer (Epoch; BioTek Instruments, Inc.).

Wound-healing assay. When the cell density of the 6-well plate reached ~90%, the state of the cells was observed using an inverted microscope (RCX41; Ningbo Sunny Precision Industry Co., Ltd). The cells were then scratched using a 100- μ l pipette tip, were washed three times with PBS to remove the scratched cells and incubated at 37°C in a 5% CO₂ incubator with 1% serum-containing medium (32). Images of the experimental and control groups were captured at 0 and 24 h. Image-Pro Plus 6.0 (Media Cybernetics) was used for assessing the relative width of the wound. Wound healing area was calculated as Final width/Initial width.

Flow cytometric analysis of the cell cycle and apoptosis. To assess apoptosis, PANC-1 cells were collected after 48 h of infection. PANC-1 cells were washed with PBS, followed by suspension in 1.5 ml centrifuge tube, centrifuged at 100 x g at room temperature for 5 min. After centrifugation, cells were washed with 1 ml PBS, resuspended with 100 μ l 1X binding

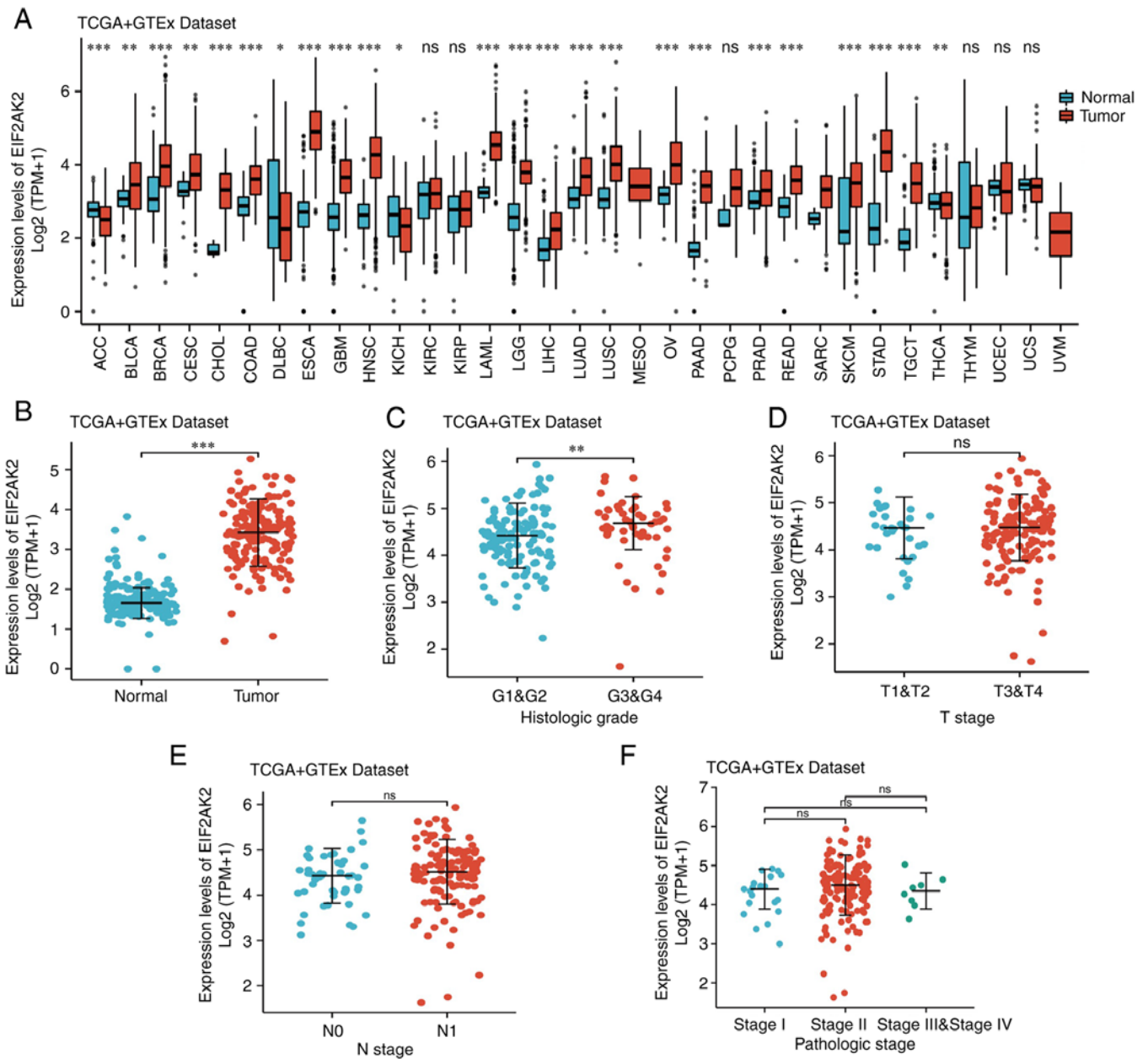


Figure 1. EIF2AK2 expression levels based on The Cancer Genome Atlas and Genomic Tumor Expression Atlas. (A) Expression levels of EIF2AK2 were different in various cancer tissues compared with those in their corresponding normal tissues. (B) Compared with in normal tissues, the expression levels of EIF2AK2 were significantly increased in pancreatic carcinoma tissues. (C) Association between EIF2AK2 and clinical manifestation; higher EIF2AK2 expression was associated with higher histological grade. There was no statistically significant difference in EIF2AK2 mRNA expression levels between the (D) T stage, (E) N stage and (F) pathological stage groups. * $P < 0.05$, ** $P < 0.01$, *** $P < 0.001$, EIF2AK2, eukaryotic translation initiation factor 2 α kinase 2; ns, not significant; TPM, transcripts per million.

buffer, and filtered through a 70 μ m cell sieve. PE staining solution (5 μ l) was added and incubated at room temperature for 5 min, then 7-AAD staining solution (10 μ l) added and incubated at room temperature for 20 min. Finally, the apoptosis rate (percentage of early apoptotic + late apoptotic cells) was examined using flow cytometry (CytOFLEX; Beckman Coulter, Inc.) and analysis with CytExpert software v.2.4 (Beckman Coulter, Inc.). Annexin-V PE/7-AAD/Apoptosis Detection Kit (cat. no. CA1030) was purchased from Beijing Solarbio Science & Technology Co., Ltd.

To assess the cell cycle, following infection PANC-1 cells were washed with PBS to collect cell suspension in 1.5 ml centrifuge tube, centrifuged at 100 x g at room temperature

for 5 min. Cells were collected by adding 1 ml PBS to be washed again, and 500 μ l 70% ethanol was added to fix the cells at room temperature for 2 h. Centrifugation was carried out at 100 x g at room temperature for 5 min. PBS (1 ml) was added to wash off the residual fixation solution. RNase A solution (100 μ l) was added to resuspend the cells at 37°C for 30 min. PI staining solution (400 μ l) was added, mixed well and incubated at 4°C in the dark for 30 min. Finally, the cell cycle was detected with a flow cytometer (CytOFLEX, Beckman Coulter, Inc.) and analyzed with CytExpert software v.2.4 (Beckman Coulter, Inc.). DNA Content Quantitation Assay (Cell Cycle; cat. no.: CA1510) purchased from Beijing Solarbio Science & Technology Co., Ltd.

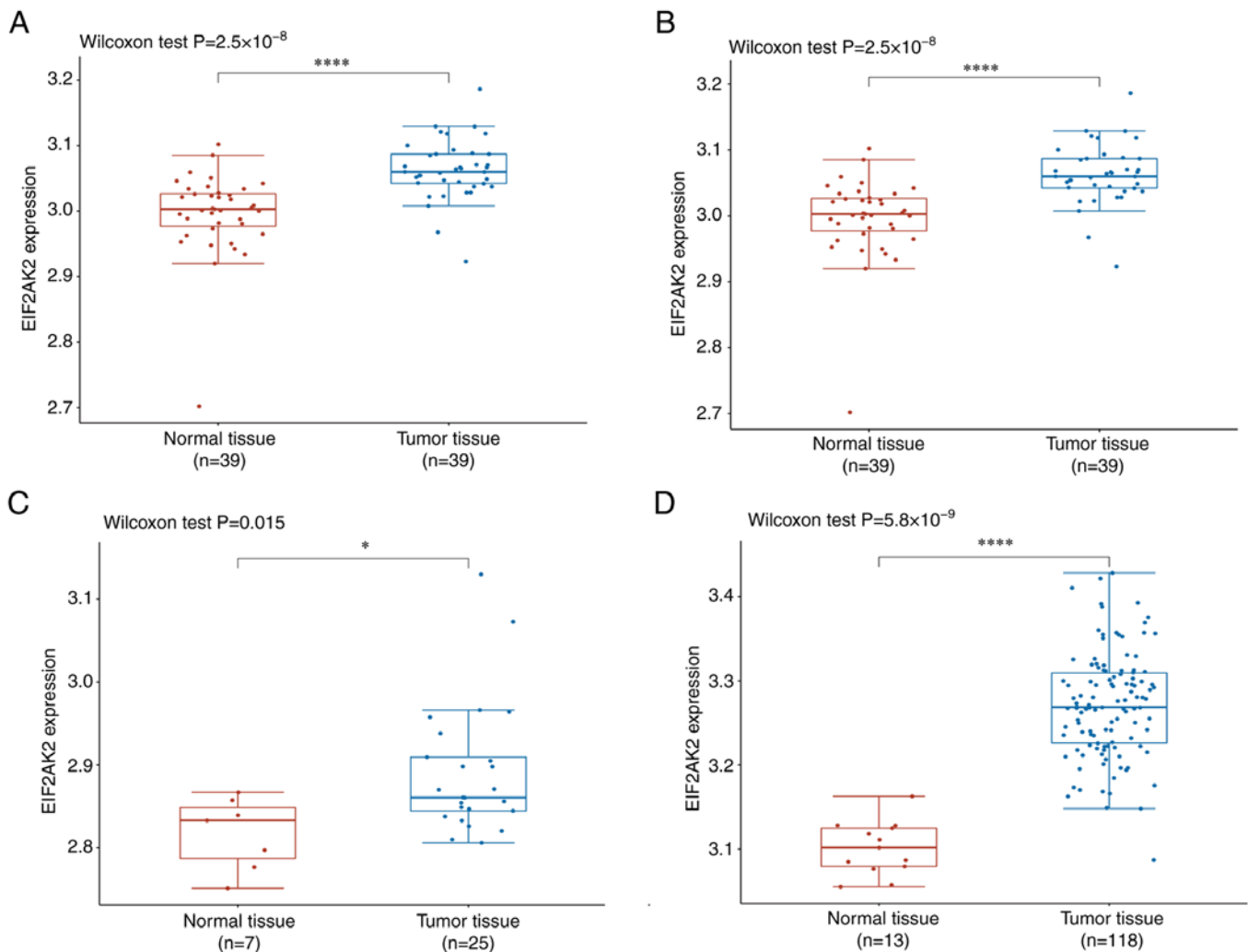


Figure 2. Aberrant expression of EIF2AK2 based on the Gene Expression Omnibus database. EIF2AK2 mRNA levels in pancreatic carcinoma tissues and normal tissues in the (A) GSE15471, (B) GSE16515, (C) GSE32676 and (D) GSE62165 datasets. *P<0.05, ****P<0.0001. EIF2AK2, eukaryotic translation initiation factor 2 α kinase 2 tissues.

Prognostic analysis. First, survival studies of overall survival (OS) and disease-specific survival (DSS) were performed to elucidate the prognostic value of EIF2AK2. In TCGA dataset, RNA sequencing data and accompanying clinical data were gathered and visualized using receiver operating characteristic (ROC) and Kaplan-Meier curves. Pancreatic cancer patients were categorized into low-risk and high-risk groups based on the median expression of EIF2AK2. P-values and hazard ratios (HR) and 95% confidence intervals (CI) were derived by log-rank test and univariate Cox proportional hazards regression. The association between EIF2AK2 expression, and OS and DSS rates in patients with pancreatic carcinoma from TCGA database was also assessed using univariate and multivariate regression models. Finally, a personalized nomogram was drawn up to predict the OS and DSS of patients with malignant neoplasms of the pancreas, which comprises calibration plots and critical clinical data.

Functional enrichment analysis. The differential expression of EIF2AK2 in pancreatic cancer data in the TCGA database was assessed using the limma package (<https://bioconductor.org/packages/release/bioc/html/limma.html>, v.4.3). To account

for false-positive results, adjusted P-values were used. Adjusted P<0.05 and \log_2 (fold change)>1 were established as criteria for distinguishing differentially expressed genes (DEGs). The results of this analysis were analyzed using the ClusterProfiler package (<https://bioconductor.org/packages/clusterProfiler/>; v.3.14.3) for Gene Ontology (GO) and the Kyoto Encyclopedia of Genes and Genomes (KEGG) to further determine the crucial biological functions of EIF2AK2.

Gene set enrichment analysis (GSEA). To examine functional and pathway differences between the EIF2AK2 high and low expression groups (33), GSEA analyses of GSE15471 in the GEO database were performed using ClusterProfiler. According to the median expression of EIF2AK2, samples were classified as high or low EIF2AK2 levels. The gene sets were sorted 1,000 times for each analysis to obtain more accurate results. Adjusted P-values <0.05 and FDR values <0.25 were considered statistically significant.

Immune cell infiltration and immune checkpoints correlated with EIF2AK2. TIMER (<https://cistrome.shinyapps.io/timer/>; v.2.0) was used to examine the correlation of EIF2AK2

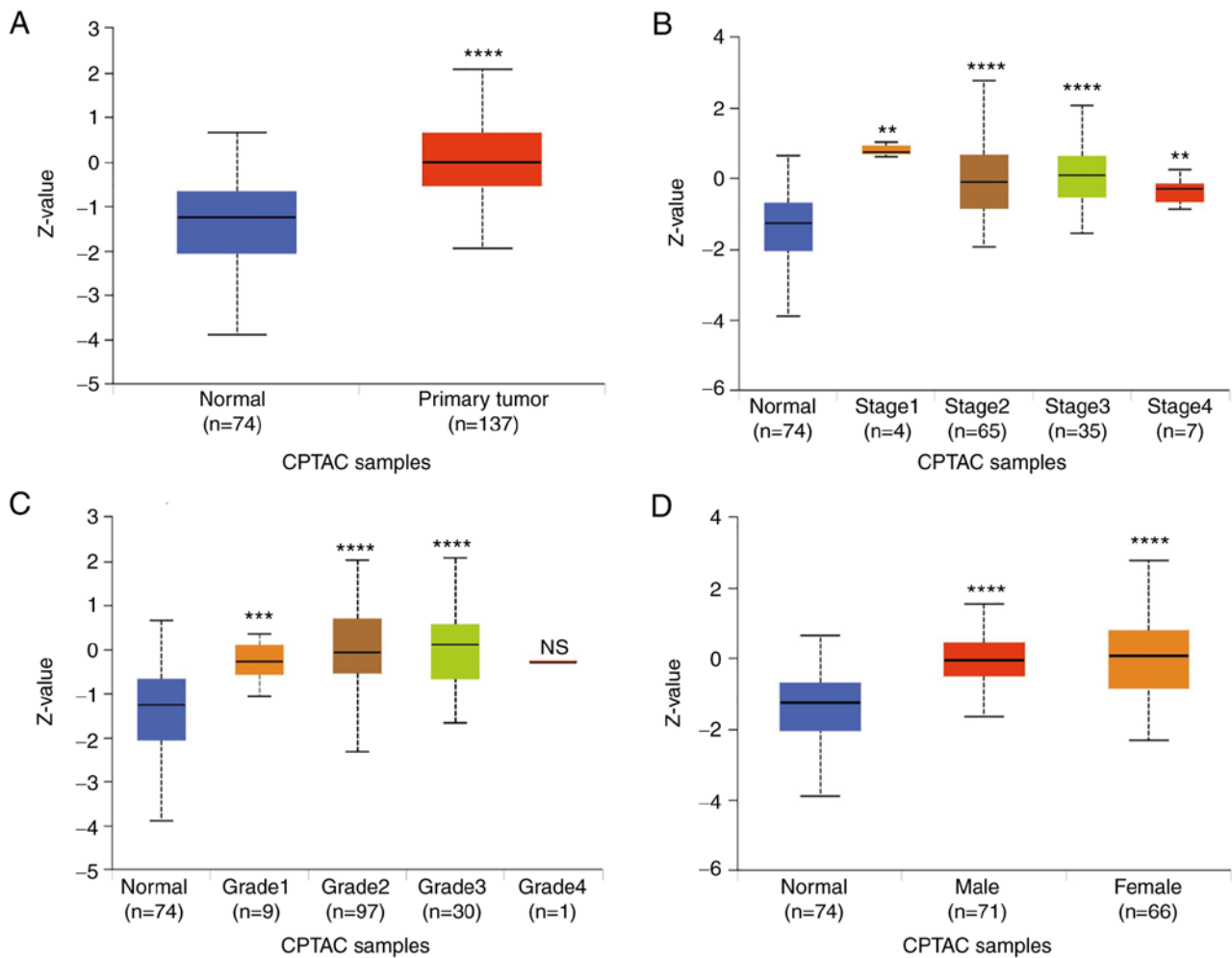


Figure 3. Analysis of EIF2AK2 protein expression using the UALCAN database. (A) Protein expression analysis of EIF2AK2. (B) Protein expression levels of EIF2AK2 were compared in different TNM stages. (C) Protein expression levels of EIF2AK2 were compared in different tumor grades. (D) Protein expression levels of EIF2AK2 were compared between the sexes. ** $P < 0.01$, *** $P < 0.001$, **** $P < 0.0001$ vs. the respective control. EIF2AK2, eukaryotic translation initiation factor 2 α kinase 2; NS, no significance. CPTAC, Clinical Proteomic Tumor Analysis Consortium.

expression with immune cell infiltration and immune cell biomarkers. Immunological infiltration analysis of EIF2AK2 was performed by single-sample gene set enrichment analysis (ssGSEA) using the GSVA (<https://github.com/rcastelo/GSVA>; v.4.3) package in R. A total of 24 infiltrating immune cells were analyzed for correlation with EIF2AK2. Finally, the association between EIF2AK2 expression and pancreatic cancer immune checkpoints was evaluated. $P < 0.05$ was considered to indicate a statistically significant difference.

Statistical methods. R (<https://www.r-project.org/>; v.3.6.3) and SPSS (IBM Corp.; v.23.0.) were used to perform statistical analysis. Experimental data from three replicates are presented as the mean \pm standard deviation. Comparisons between two groups were made using paired two-tailed Student's t-test, and comparisons between multiple groups were made using one-way ANOVA with Dunnett's post-hoc test. Pearson χ^2 test was used to analyze the association between EIF2AK2 expression levels and clinicopathological characteristics. Cox regression and Kaplan-Meier analyses were used to evaluate prognostic factors. Multi-factorial Cox analysis was used to compare the effect of EIF2AK2 expression and other clinical characteristics

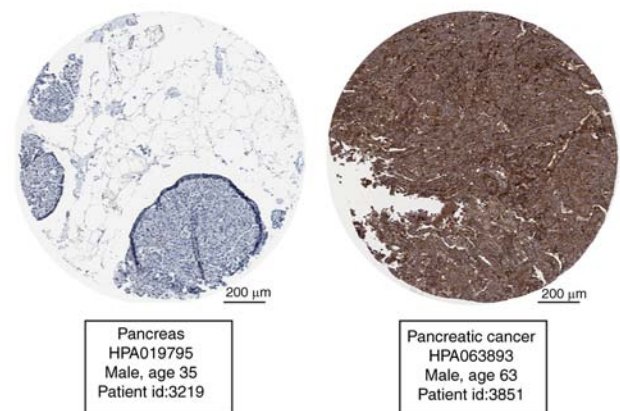


Figure 4. Representative immunohistochemistry images and detailed information on the expression of eukaryotic translation initiation factor 2 α kinase 2 in pancreatic carcinoma tissues and normal tissues based on The Human Protein Atlas database.

on survival. Median EIF2AK2 expression was used as the cut-off value. In addition, ROC analysis was performed using the pROC package (<https://www.rdocumentation>.

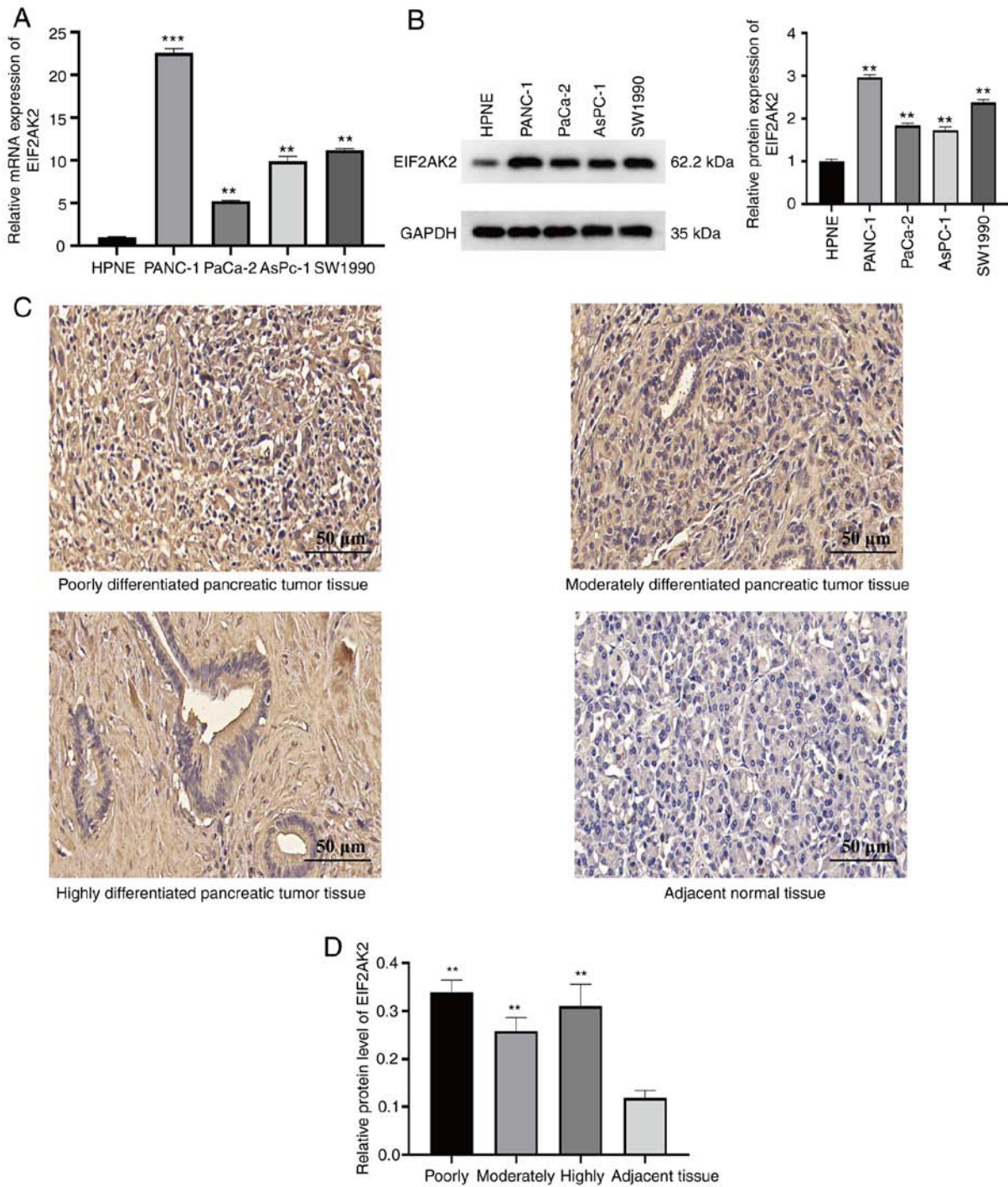


Figure 5. EIF2AK2 is upregulated in pancreatic carcinoma. (A) mRNA level and (B) protein expression of EIF2AK2 using reverse transcription-quantitative PCR and western blotting, respectively. **P<0.01, ***P<0.001 vs. HPNE. (C and D) Low and high expression of EIF2AK2 in differently differentiated pancreatic cancer tissues and adjacent tumour tissues. **P<0.01 vs. adjacent tissue; Scale bar, 50 μm; EIF2AK2, eukaryotic translation initiation factor 2α kinase 2; poorly, poorly differentiated pancreatic tumour tissue; moderately, moderately differentiated pancreatic tumour tissue; highly, highly differentiated pancreatic tumour tissue.

org/packages/pROC/versions/1.17.0.1; v.1.17.0.1) to assess the effectiveness of EIF2AK2 transcript expression in differentiating between pancreatic cancer and healthy samples. Area under the curve (AUC) values were calculated between 0.5-1.0, indicating an identification capacity of 50-100%. Spearman's test was used to analyze the correlation between EIF2AK2 expression levels and immune cell infiltration. P<0.05 was considered to indicate a statistically significant difference in all tests.

Results

EIF2AK2 expression is elevated in pancreatic cancer. The results of pancancer analysis of EIF2AK2 revealed that the mRNA expression levels of EIF2AK2 were increased in adrenocortical carcinoma, bladder urothelial carcinoma, breast invasive carcinoma, cholangiocarcinoma, colon adenocarcinoma/rectal adenocarcinoma, esophageal carcinoma, glioblastoma multiforme, liver hepatocellular carcinoma, lung

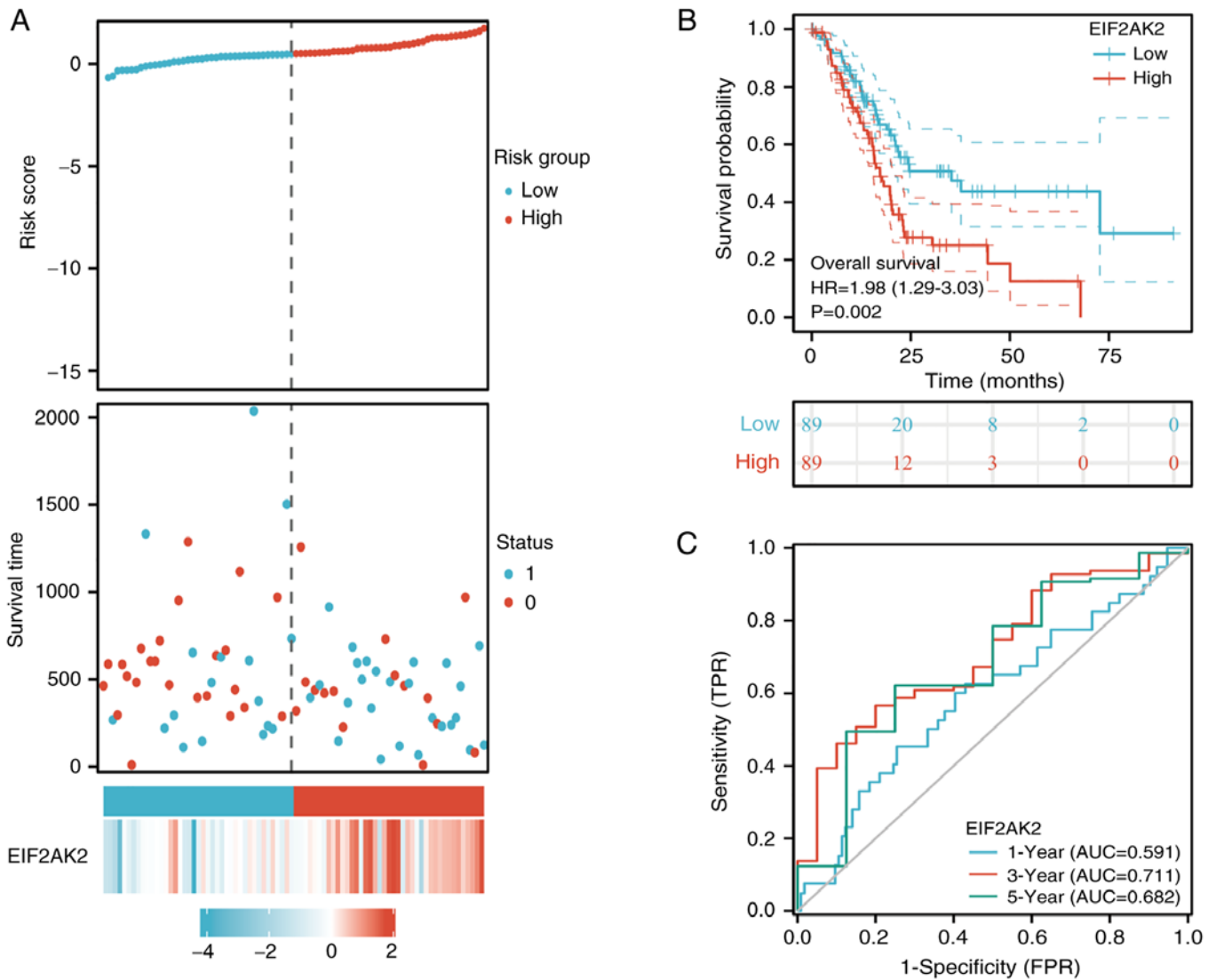


Figure 6. Prognostic analysis of EIF2AK2 expression on overall survival in pancreatic carcinoma. (A) Survival curve of EIF2AK2 expression. (B) Receiver operating characteristic curve of EIF2AK2 expression. (C) EIF2AK2 expression distribution, survival status and heatmap of the EIF2AK2 expression profiles. EIF2AK2, eukaryotic translation initiation factor 2 α kinase 2; 1, dead; 0, alive; AUC, area under the curve; TPR, True positive fraction; FPR, False positive fraction.

squamous cell carcinoma, rectal adenocarcinoma, thyroid carcinoma, lung adenocarcinoma, prostate adenocarcinoma and pancreatic adenocarcinoma (Fig. 1A). After removing the samples with zero expression value, combined with pancreatic cancer samples from the TCGA database and normal pancreatic tissue samples from the GTEx database, the results showed that the expression level of EIF2AK2 was significantly elevated in pancreatic cancer tissues when compared to normal pancreatic tissues (tumor: 3.21 ± 0.85 , normal: 1.20 ± 0.55 , $P < 0.0001$; Fig. 1B). Further analysis indicated statistically significant differences in EIF2AK2 expression between histological grades ($P < 0.05$), but not between T, N or pathological stages ($P > 0.05$; Fig. 1C-F).

The higher expression of EIF2AK2 in pancreatic tumor tissues compared with normal pancreatic tissues was verified in the GSE15471, GSE16515, GSE32676 and GSE62165 datasets. ($P < 0.05$; Fig. 2). In addition, the expression of EIF2AK2 was analyzed in the UALCAN online tumor database website, where high EIF2AK2 expression was associated with gene

expression, tumor grade, stage and gender in patients with pancreatic cancer (Fig. 3). Subsequently, THPA database was used to verify EIF2AK2 expression in pancreatic cancer and normal tissues. The expression levels of EIF2AK2 in pancreatic cancer tissues were substantially higher compared with those in normal tissues (Fig. 4).

To validate EIF2AK2 expression in pancreatic cancer cells *in vitro*, normal pancreatic cells were compared with four distinct pancreatic cancer cell lines. RT-qPCR and western blotting results indicated that the pancreatic cancer cell lines had significantly higher mRNA and protein expression levels of EIF2AK2 compared with those in normal pancreatic cells (Fig. 5A and B). To further examine the expression characteristics of EIF2AK2 in pancreatic carcinoma, immunohistochemical staining of pancreatic tumor tissues and adjacent normal tissues from 48 patients was performed. Notably, EIF2AK2 was revealed to be localized in the nucleus. The results showed that EIF2AK2 was weakly positive in paraneoplastic tissues, but was highly expressed in pancreatic cancer

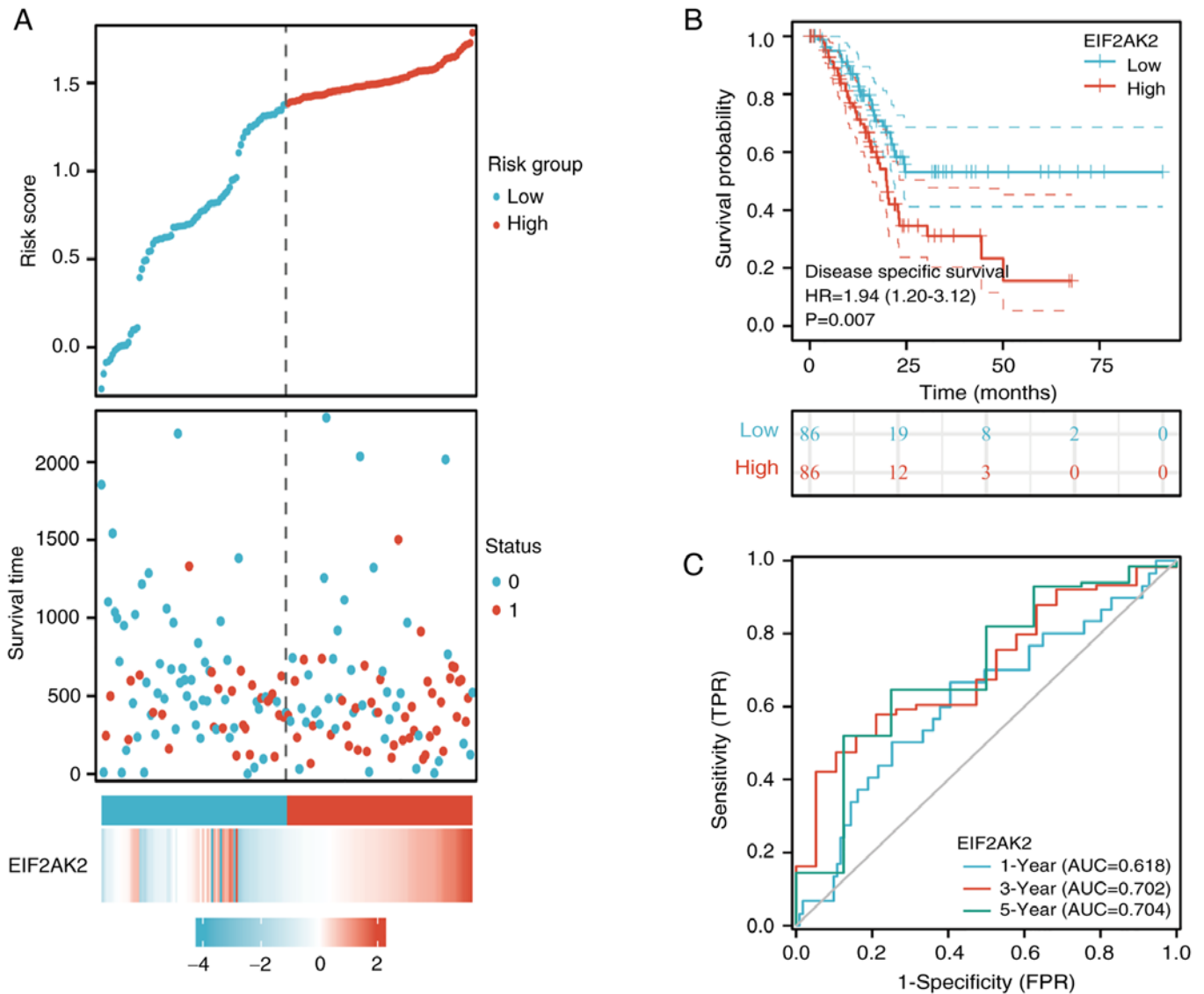


Figure 7. Prognostic analysis of EIF2AK2 expression on disease-specific survival in pancreatic carcinoma. (A) Survival curve of EIF2AK2 expression. (B) Receiver operating characteristic curve of EIF2AK2 expression. (C) EIF2AK2 expression distribution, survival status and heatmap of the EIF2AK2 expression profiles. EIF2AK2, eukaryotic translation initiation factor 2 α kinase 2; 1, dead; 0, alive; AUC, area under the curve; TPR, True positive fraction; FPR, False positive fraction.

tissues (Fig. 5C). Furthermore, as shown in Fig. 5D, EIF2AK2 expression was considerably higher in highly, moderately and poorly differentiated pancreatic cancer compared with that in adjacent pancreatic tissues. These findings indicated that EIF2AK2 may be highly expressed in pancreatic cancer.

Prognostic relevance of EIF2AK2. To predict the relationship between EIF2AK2 expression level and survival in patients with pancreatic cancer, the link between EIF2AK2 expression and the prognosis of patients with pancreatic cancer was evaluated. Notably, the expression of EIF2AK2 was substantially linked with OS in patients with pancreatic cancer. Based on median EIF2AK2 expression, patients were separated into high expression and low expression groups. Combining the risk profile and survival status, it was found that the fatality rate was considerably greater in the EIF2AK2 high-expression group compared with that in the low-expression group. Considering the risk profile and survival together, the mortality rate in the

EIF2AK2 high-expression group was significantly higher than that in the low-expression group (Fig. 6A). High expression of EIF2AK2 was substantially linked with a poor prognosis, based on the Kaplan-Meier survival analysis (HR=1.98, 95% CI=1.29-3.03, P=0.002; Fig. 6B). To observe the predictive value of EIF2AK2 mRNA expression in prognosis, EIF2AK2 expression was assessed using ROC curves to distinguish between EIF2AK2-high and EIF2AK2-low patients. It was determined that evaluating the area under the curve (AUC) under the ROC curve to estimate the risk of patients with pancreatic cancer at 1, 3 and 5 years was the most effective measure (1-year AUC, 0.591; 3-year AUC, 0.711; 5-year AUC, 0.682) (Fig. 6C).

In addition, the relationship between EIF2AK2 expression and DSS in patients with pancreatic cancer was analyzed. Considering the risk profile and survival together, the mortality rate in the EIF2AK2 high-expression group was significantly higher than that in the low-expression

Table I. Association of EIF2AK2 expression and other clinicopathological factors with OS calculated via univariate and multivariate Cox regression analyses.

Characteristic	Univariate analysis			Multivariate analysis		
	N	HR (95% CI)	P-value	N	HR (95% CI)	P-value
T stage	176		0.03	176		0.249
T1 and T2	31	Reference		31	Reference	
T3 and T4	145	2.023 (1.072-3.816)		145	1.798 (0.663-4.877)	
N stage	173		0.004	173		0.04
N0	50	Reference		50	Reference	
N1	123	2.154 (1.282-3.618)		123	1.969 (1.033-3.753)	
Pathological stage	175		0.037	175		0.307
Stage I	21	Reference		21	Reference	
Stage II, Stage III and Stage IV	154	2.291 (1.051-4.997)		154	0.491 (0.125-1.926)	
Sex	178		0.311			
Female	80	Reference				
Male	98	0.809 (0.537-1.219)				
Age	178		0.227			
≤65 years	93	Reference				
>65 years	85	1.290 (0.854-1.948)				
Histological grade	176		0.052			
G1 and G2	126	Reference				
G3 and G4	50	1.538 (0.996-2.376)				
EIF2AK2	178		0.002	178		0.042
Low	89	Reference		89	Reference	
High	89	1.981 (1.294-3.032)		89	1.585 (1.017-2.470)	

EIF2AK2, eukaryotic translation initiation factor 2 α kinase 2; OS, overall survival; HR, hazard ratio; CI, confidence interval.

group (Fig. 7A). The assessment of the connection between EIF2AK2 expression and DSS illustrated that EIF2AK2 expression not only affected the DSS of patients with pancreatic cancer (HR=1.94, 95% CI=1.20-3.12, P=0.007; Fig. 7B) but also predicted overall risk (1-year AUC, 0.618; 3-years AUC, 0.702; 5-year AUC,=0.704; Fig. 7C). Taken together, these consistent OS and DSS outcomes strongly indicated that the EIF2AK2 gene is related to the prognosis of patients with pancreatic cancer.

In addition, as shown in Table I, the univariate Cox analysis revealed that high EIF2AK2 levels, and high T, N and pathological stages were associated with OS (P<0.05). In the multivariate Cox analysis, N stage and EIF2AK2 expression represented independent components associated with OS in patients with pancreatic cancer. Similarly, as shown in Table II, the univariate Cox analysis revealed that high EIF2AK2 levels, and high T, N and pathological stages were associated with DSS events (P<0.05). In the multivariate Cox analysis, only N stage was an independent factor associated with DSS in patients with pancreatic cancer.

Through the integration of clinicopathological factors (including T stage, N stage, pathological stage and EIF2AK2 expression), a nomogram model was generated from the results of the OS and DSS analyses, which can be employed to accurately measure the survival probabilities at 1-, 3- and 5-years in clinical settings (Fig. 8).

Functional inference of EIF2AK2. To further confirm the putative biological roles of the EIF2AK2 gene, a functional enrichment analysis was performed using TCGA transcriptome data. Based on the degree of EIF2AK2 expression, pancreatic cancer samples were categorized as EIF2AK2^{high} or EIF2AK2^{low}. Next, the DEGs analyzed in the EIF2AK2^{high} and EIF2AK2^{low} groups were identified using the following criteria: $|\log_2FC| > 1$, adjusted P<0.05. A total of 1,318 genes exhibited different expression levels, 209 upregulated genes and 1,109 downregulated genes, as indicated by the volcano plot (Fig. 9A). These degrees were analyzed using a heatmap for hierarchical clustering (Fig. 9B). To determine the possible function of EIF2AK2, a range of enrichment analyses were performed, including GO and KEGG. The GO enrichment analysis included three main functions, namely, biological process, cellular components, and molecular functions. The biological process mainly included fat digestion and absorption, Pancreatic secretion, protein digestion and absorption, salivary secretion, digestion antimicrobial humoral response, response to food. Molecular functions mainly included antigen binding, receptor ligand activity, immunoglobulin receptor binding, humoral immune response, humoral immune response mediated by circulating immunoglobulin, serine hydrolase activity, serine-type peptidase activity, serine-type endopeptidase activity. Cellular components mainly included immunoglobulin complex, external side of plasma membrane,

Table II. Association of EIF2AK2 expression and other clinicopathological factors with DSS in pancreatic cancer calculated via univariate and multivariate Cox regression analyses.

Characteristic	Univariate analysis			Multivariate analysis		
	N	HR (95% CI)	P-value	N	HR (95% CI)	P-value
T stage	170		0.008	170		0.1
T1 and T2	30	Reference		30	Reference	
T3 and T4	140	3.119 (1.346-7.229)		140	3.210 (0.800-12.875)	
N stage	167		0.001	167		0.024
N0	48	Reference		48	Reference	
N1	119	2.746 (1.473-5.121)		119	2.368 (1.120-5.004)	
Pathological stage	169		0.023	169		0.297
Stage I	20	Reference		20	Reference	
Stage II, Stage III and Stage IV	149	3.249 (1.175-8.979)		149	0.379 (0.061-2.347)	
Sex	172		0.227			
Female	76	Reference				
Male	96	0.715 (0.473-1.194)				
Age	172		0.784			
≤65 years	92	Reference				
>65 years	80	1.067 (0.670-1.701)				
Histological grade	170		0.053			
G1 and G2	122	Reference				
G3 and G4	48	1.616 (0.994-2.628)				
EIF2AK2	172		0.007	172		0.157
Low	86	Reference		86	Reference	
High	86	1.935 (1.202-3.115)		86	1.425 (0.872-2.329)	

EIF2AK2, eukaryotic translation initiation factor 2 α kinase 2; DSS, disease-specific survival; HR, hazard ratio; CI, confidence interval.

immunoglobulin complex, circulating, neuron projection membrane, dendrite membrane, AMPA glutamate receptor complex. KEGG analysis demonstrated that EIF2AK2 might regulate the process of complement activation, classical pathway. Obviously, GO and the KEGG results can be concluded to provide a new direction for tumor immunotherapy research (Fig. 9C and D). Fig. 9E shows the GSEA of all genes significantly coexpressed with EIF2AK2. Notably, the functions of these genes significantly coexpressed with EIF2AK2 were mainly enriched in the cell cycle, degradation of extracellular matrix, complement system and activation of extracellular goblet B cells by Sarscov2.

Association between EIF2AK2 expression and biomarkers of immune cells. To investigate the relevance of EIF2AK2 in the tumor immune microenvironment, correlations were established between EIF2AK2 expression and immune cell biomarkers. As listed in Table III, EIF2AK2 was positively correlated with B-cell biomarkers (CD19, CD20 and CD38), CD8⁺ T-cell biomarkers (CD8A and CD8B), other T-cell subsets [follicular helper T cells, T helper (Th)1, Th2, Th9, Th17, Th22 and regulatory T cells (Tregs)], M1 macrophage biomarkers (IRF5 and PTGS2), M2 macrophage biomarkers (CD115), tumor-associated macrophage (TAM) biomarkers (PDCD1LG2, CD80, CD40 and TLR7), natural killer cell biomarkers (CD7 and XCL1), neutrophil biomarkers (ITGAM

and FUT4) and dendritic cell (DC) biomarkers (CD1C and ITGAX) in pancreatic cancer. These findings indicated the existence of a direct relationship between EIF2AK2 and immune cell invasion.

Immune infiltration analysis. The correlation of EIF2AK2 expression with immune cell infiltration into the microenvironment of pancreatic cancer tumors was quantified by ssGSEA, as calculated by Spearman correlation analysis. EIF2AK2 expression was weakly associated with the StromalScore, ImmuneScore and the ESTIMATE score (Fig. 10B-D). Notably, EIF2AK2 was correlated with activated DCs (aDCs), T cells, CD4⁺ T-cell subsets (Th1 cells, Th2 cells, Tregs, Th17 cells, follicular helper T cells), CD8⁺ T cells, $\gamma\delta$ T cells, memory T-cell subsets [central memory T (Tcm) cells, effective memory T cells], T helper cells, B cells, macrophages, eosinophils, mast cells, neutrophils, DCs, immature DCs, plasmacytoid DCs (pDCs), natural killer (NK) cells, NK cell subsets (NK CD56dim cells and NK CD56bright cells) and cytotoxic cells (Fig. 10A).

Relationship between EIF2AK2 expression and immune checkpoints. To determine the relationship between EIF2AK2 expression and immune cell, the interactions between EIF2AK2 and chemokines and chemokine receptors were studied. It was revealed that there was a significant correlation

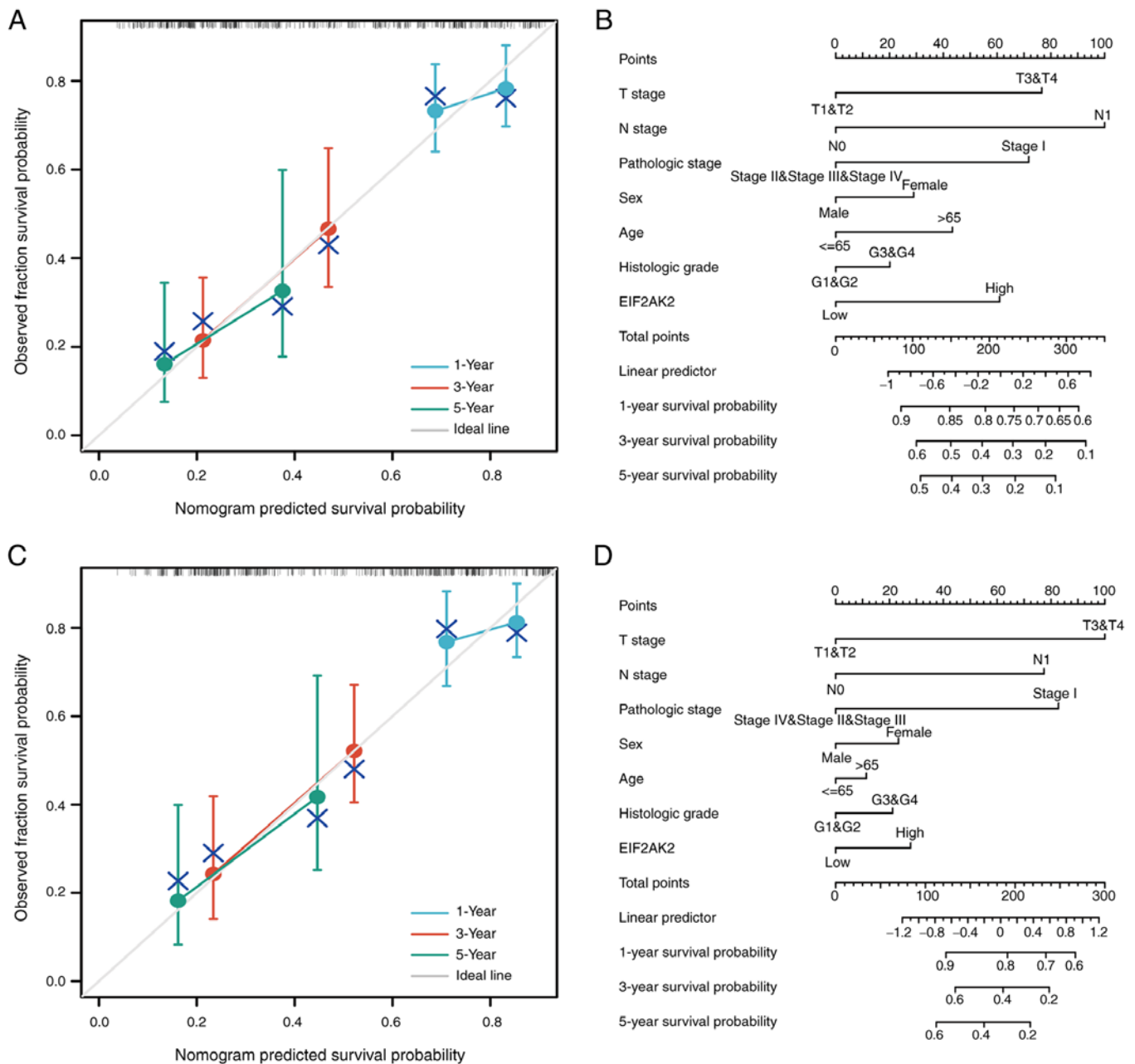


Figure 8. A prognostic predictive model of EIF2AK2 in pancreatic carcinoma. (A) Nomogram for predicting the probability of 1-, 3-, 5-year OS. (B) Calibration plot of the nomogram for predicting the probability of OS at 1, 3 and 5 years. (C) Nomogram for predicting the probability of 1-, 3-, 5-year DSS. (D) Calibration plot of the nomogram for predicting the probability of DSS at 1, 3 and 5 years. EIF2AK2, eukaryotic translation initiation factor 2 α kinase 2; OS, overall survival; DSS, disease-specific survival.

between the expression of EIF2AK2 and immune cell-associated chemokines, as well as chemokine receptors, such as CTLA4 ($r_s=0.311$, $P<0.001$), HAVCR2 ($r_s=0.423$, $P<0.001$), LAG3 ($r_s=0.207$, $P=0.006$), PDCD1 ($r_s=0.221$, $P=0.003$), CD274 ($r_s=0.601$, $P\leq 0.001$), PDCD1LG2 ($r_s=0.501$, $P<0.001$) and TIGIT ($r_s=0.341$, $P<0.001$) (Fig. 11). Since the expression of these chemokines and chemokine receptors appears to be correlated with EIF2AK2 expression, it is possible that high EIF2AK2 expression is implicated in the migration of immune cells to the tumor microenvironment. Spearman correlation analysis showed that LAG3 and PDCD1 were weakly correlated with EIF2AK2 and the others were moderately correlated with it.

EIF2AK2 knockdown inhibits the migration and proliferation of PANC-1 cells. The present study revealed that EIF2AK2 was upregulated in pancreatic cancer and that it was negatively associated with the survival of patients with pancreatic cancer; however, the role of EIF2AK2 in pancreatic carcinogenesis requires further investigation. Three EIF2AK2 shRNA knockdown vectors were constructed and transfected into PANC-1 cells. The effect of lentiviral infection is shown in Fig. S1A. RT-qPCR results showed that sh-EIF2AK2-397 (Shanghai GeneChem Co., Ltd. cat. no. 115397-1) was more efficient than sh-EIF2AK2-396 (Shanghai GeneChem Co., Ltd. cat. no. 115396-2) and sh-EIF2AK2-398 (Shanghai GeneChem Co., Ltd. cat. no. 115398-1) (Fig. S1B). Therefore,

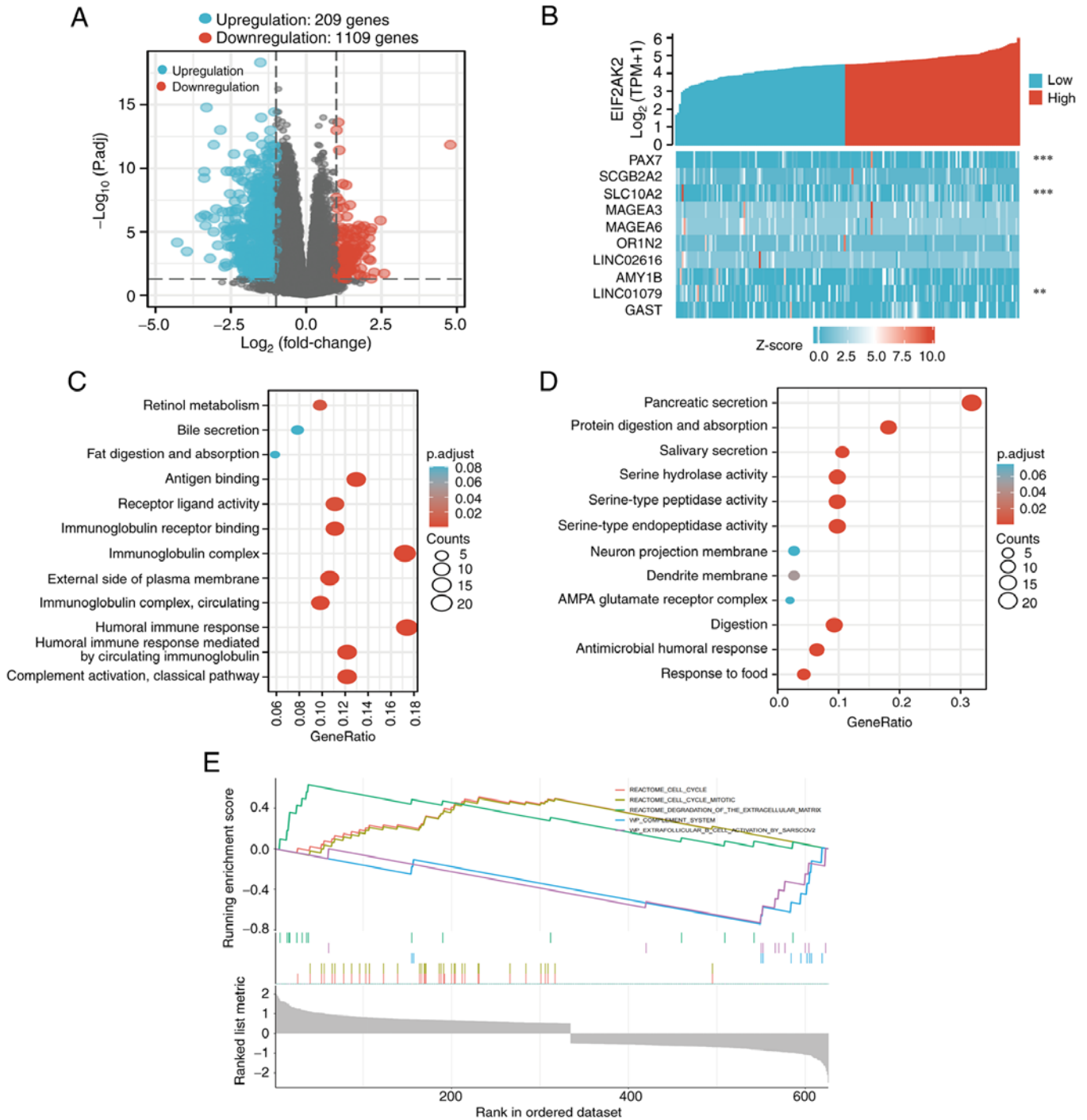


Figure 9. A total of 1,318 DEGs were identified as being statistically significant between EIF2AK2 high-expression and low-expression groups. (A) Volcano plot of DEGs, including 209 upregulated and 1,109 downregulated genes. Normalized expression levels were shown in descending order from blue to red. (B) Heatmap of the 10 DEGs, including five upregulated genes and five downregulated genes. The x-axis represents the samples, while the y-axis denotes the DEGs. Blue and red represent downregulated and upregulated genes, respectively. **P<0.01, ***P<0.001 vs. EIF2AK2. The X-axis represents the samples, while the Y-axis denotes the differentially expressed RNAs. Blue and red tones represented down-regulated and up-regulated genes, respectively. (C) KEGG enrichment and GO enrichment analysis of EIF2AK2 coexpressed upregulated DEGs. (D) KEGG enrichment and GO enrichment analysis of EIF2AK2 coexpressed downregulated DEGs. (E) Enrichment plots from the gene set enrichment analysis. DEGs, differentially expressed genes; EIF2AK2, eukaryotic translation initiation factor 2 α kinase 2; KEGG, Kyoto Encyclopedia of Genes and Genomes; GO, Gene Ontology.

subsequent *in vitro* cellular experiments were performed using sh-EIF2AK2-397. To investigate whether EIF2AK2 affects the proliferation and migration of PANC-1 cells, CCK-8 and wound-healing assays were performed. As shown in Fig. 12A and B, the knockdown of EIF2AK2 markedly diminished PANC-1 cell proliferation and migration. These results

confirm that EIF2AK2 promotes PANC-1 cell proliferation and migration

Effect of EIF2AK2 knockdown on PANC-1 cell cycle progression and apoptosis. The present study further assessed the effect of EIF2AK2 expression on apoptosis and cell cycle

Table III. Correlation analysis between EIF2AK2 expression and immune cell markers.

Immune cell	Biomarker	Spearman's r_s value	P-value
TAM	PDCD1LG2	0.510	<0.001
	CD80	0.490	<0.001
	CD40	0.296	<0.001
	TLR7	0.394	<0.001
Natural killer cell	CD7	0.159	0.034
	KIR3DL1	-0.040	0.593
	XCL1	0.265	<0.001
Neutrophil	CD11b (ITGAM)	0.366	<0.001
	CD15 (FUT4)	0.326	<0.001
	CD66b (CEACAM8)	0.185	0.013
Dendritic cell	CD1C	0.201	0.007
	CD11c (ITGAX)	0.243	0.001
	CD141 (THBD)	0.339	<0.001
M1 macrophage	COX2 (PTGS2)	0.424	<0.001
	INOS (NOS2)	0.207	0.006
	IRF5	0.285	<0.001
M2 macrophage	ARG1	0.014	0.851
	CD206 (MRC1)	0.353	<0.001
	CD115 (CSF1R)	0.373	<0.001
B cell	CD19	0.180	0.017
	CD20 (KRT20)	0.185	0.014
	CD38	0.363	<0.001
CD8 ⁺ T cell	CD8A	0.323	<0.001
	CD8B	0.301	<0.001
Tfh	BCL6	0.468	<0.001
	ICOS	0.359	<0.001
	CXCR5	0.180	0.016
Th1	T-bet (TBX21)	0.191	0.011
	STAT1	0.809	<0.001
	STAT4	0.230	0.002
	IL12RB2	0.130	0.085
	WSX1 (IL27RA)	0.274	<0.001
	IFN- γ (IFNG)	0.265	<0.001
	TNF- α (TNF)	0.173	0.021
Th2	CCR3	0.364	<0.001
	GATA3	0.296	<0.001
	STAT5A	0.391	<0.001
	STAT6	0.484	<0.001
Th9	IRF4	0.296	<0.001
	PU.1 (SPI1)	0.204	0.006
	TGFBR2	0.583	<0.001
Th17	IL-17A	0.128	0.089
	IL-21R	0.356	<0.001
	IL-23R	0.202	0.007
	STAT3	0.597	<0.001
Th22	AHR	0.614	<0.001
	CCR10	-0.051	0.496
Treg	CCR8	0.480	<0.001
	CD25 (IL2RA)	0.429	<0.001
	FOXP3	0.335	<0.001

EIF2AK2, eukaryotic translation initiation factor 2 α kinase 2; TAM, tumor-associated macrophage; Treg, regulatory T cell, Tfh, follicular helper T cell; Th, T helper cell.

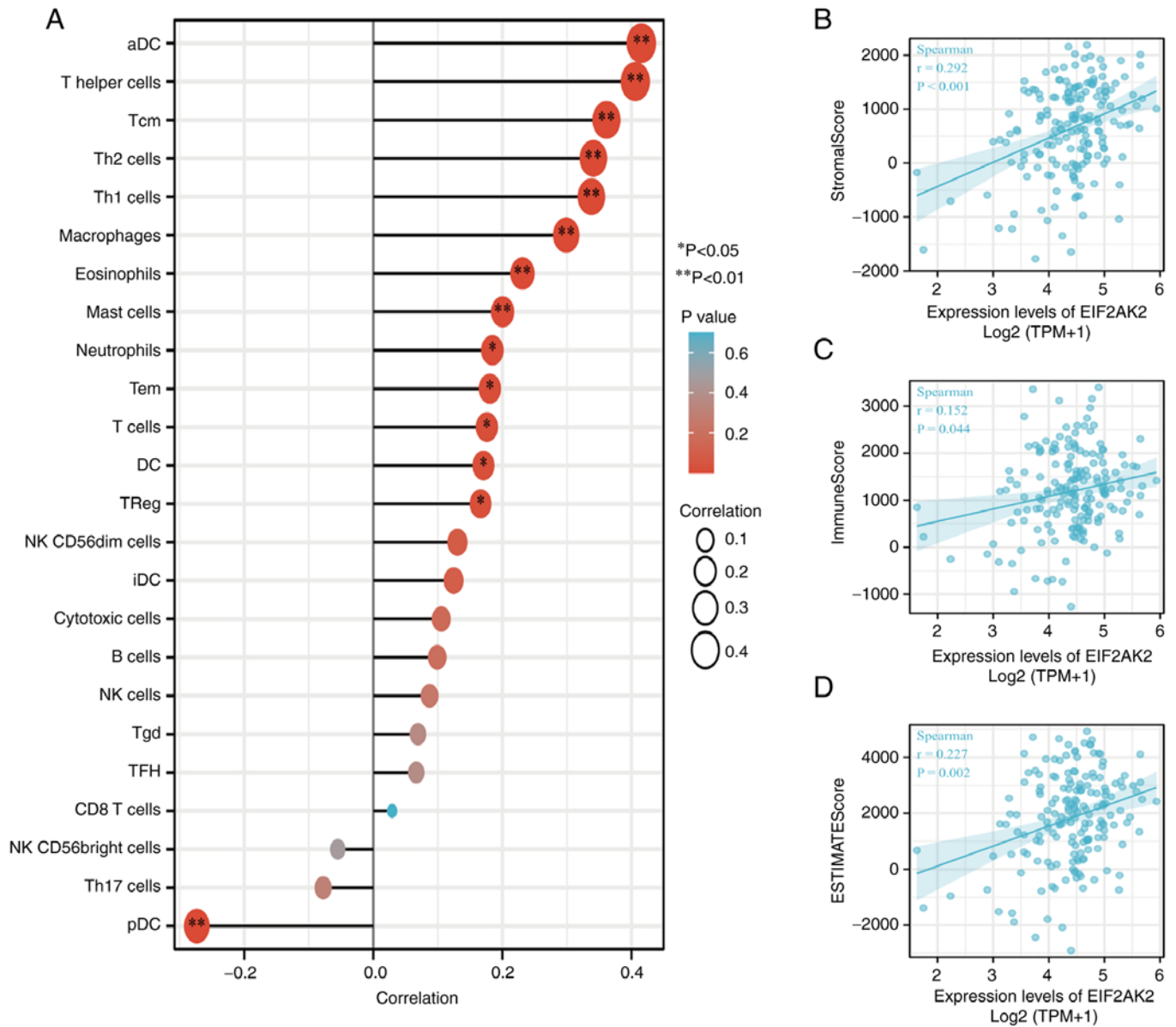


Figure 10. Expression of EIF2AK2 is associated with immune infiltration in the tumor microenvironment. (A) Correlation diagram of 24 infiltrating immune cells. (B) StromaScore, (C) ImmuneScore and (D) ESTIMATEScore in clusters in pancreatic cancer tissues and normal tissues. EIF2AK2, eukaryotic translation initiation factor 2 α kinase 2; TPM, transcripts per million.

progression in PANC-1 cells. As shown in Fig. 13, the apoptotic rate was significantly higher in the sh-EIF2AK2 group compared with that in the control and NC groups. Furthermore, the effect of EIF2AK2 knockdown on the cell cycle progression of PANC-1 cells indicated that low EIF2AK2 expression in PANC-1 cells could inhibit the cell cycle transition from G₁ to S phase and blocked it in G₂/M phase (Fig. 14).

Activation of the AKT signaling pathway by EIF2AK2. To elucidate the relationship between EIF2AK2 and pancreatic cancer development, the expression of AKT and p-AKT in cells following knockdown of EIF2AK2 was determined by western blotting. The results showed that the p-AKT/AKT ratio was decreased following knockdown of EIF2AK2 (Fig. 15). This finding suggested that EIF2AK2 may activate the AKT signaling pathway *in vitro*.

Discussion

EIF2AK2 is a serine/threonine kinase that is normally activated by dsRNA. In addition to dsRNA, EIF2AK2 can be activated by other non-self RNAs (34). EIF2AK2 was originally associated with cellular innate immunity; dsRNA binds dsRBM1 and 2 (two dsRNA binding motifs of EIF2AK2) with high affinity (KD \approx 4 nM) to induce conformational changes upon viral invasion, resulting in the release of a kinase domain from dsRBM2 leading to apoptosis in virus-infected cells (35). In addition, EIF2AK2 was considered to be a tumor suppressor based on its proapoptotic activity. The first experimental evidence of EIF2AK2 tumor-suppressing activity was provided by a catalytically inactivated EIF2AK2 mutant that inhibited endogenous EIF2AK2 activity in a dominantly negative manner (36). Its low expression level is considered to be associated with cancer phenotypes, such as active cell

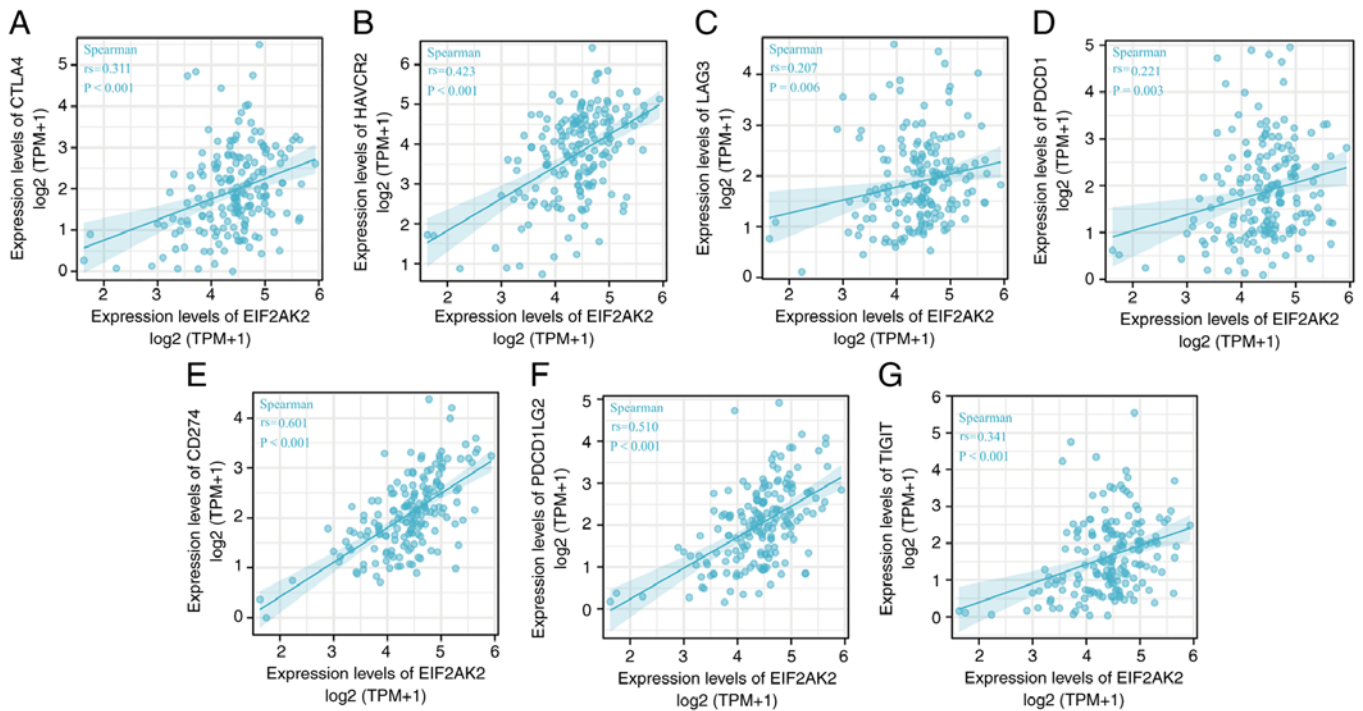


Figure 11. Correlation of EIF2AK2A expression with immune checkpoints. (A) The moderate correlation of EIF2AK2 expression with CTLA4. (B) The moderate correlation of EIF2AK2 expression with HAVCR2. (C) The weak correlation of EIF2AK2 expression with LAG3. (D) The weak correlation of EIF2AK2 expression with PDCD1. (E) The moderate correlation of EIF2AK2 expression with CD274. (F) The moderate correlation of EIF2AK2 expression with PDCD1LG2. (G) The moderate correlation of EIF2AK2 expression with TIGIT. EIF2AK2, eukaryotic translation initiation factor 2 α kinase 2; CTLA4, cytotoxic T lymphocyte-associated antigen-4; HAVCR2, Human Hepatitis A virus cellular receptor 2; LAG3, Lymphocyte activation gene 3 protein; PDCD1, Programmed cell death protein 1; CD274(also known as PD-1), programmed cell death protein 1; PDCD1LG2, Human Programmed cell death 1 ligand 2; TIGIT, T cell immunoreceptor with Ig and ITIM domains.

proliferation, poor pathological differentiation or poor patient prognosis, including in head and neck squamous cell carcinoma, breast cancer, hepatocellular carcinoma, colon cancer, bile duct cancer and primary lung cancer (37-42). Conversely, EIF2AK2 is elevated in other cancer cell subsets relative to the corresponding normal cells or tissues, and is associated with tumor aggressiveness or poor patient prognosis, including breast cancer cell lines, melanoma cells, colon cancer, thyroid cancer, hepatocellular carcinoma, bile duct cancer, acute myeloid leukemia and lung adenocarcinoma (17,40,42-46). In addition, EIF2AK2 expression shows a mixed pro-tumor and antitumor profile in a number of clinical specimens. Examples of these include breast cancer, cholangiocarcinoma and hepatocellular carcinoma samples (47).

Given the limited research conducted on the EIF2AK2 gene in cancer, to identify its biological activities and relevant regulatory mechanisms in pancreatic cancer, the present study carried out comprehensive and integrative bioinformatics research. Based on public databases and clinical samples, the first attempt to validate the expression of EIF2AK2 in pancreatic cancer tissues and its prognostic value revealed that EIF2AK2 expression was elevated in pancreatic cancer tissues compared with that in normal tissues, and that high expression was strongly associated with poorer OS and DSS in pancreatic cancer. Notably, the most clinically relevant finding was that high EIF2AK2 expression was associated with poor OS. Multivariate Cox regression analysis revealed that high EIF2AK2 expression was another independent prognostic factor in addition to N stage. Nomogram prediction modelling

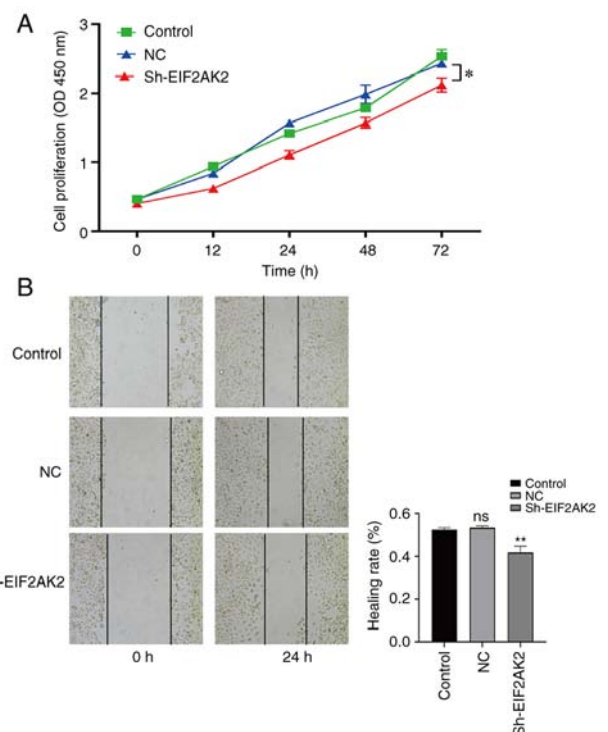


Figure 12. Knockdown of EIF2AK2 reduced the proliferation and migration of PANC-1 cells. (A) Cell Counting Kit-8 detection of cell proliferation. (B) Wound-healing assay to detect cell migration (magnification, x100). * $P < 0.05$, ** $P < 0.01$ vs. Control and NC. EIF2AK2, eukaryotic translation initiation factor 2 α kinase 2; ns, not significant; NC, negative control; Si, small interfering.

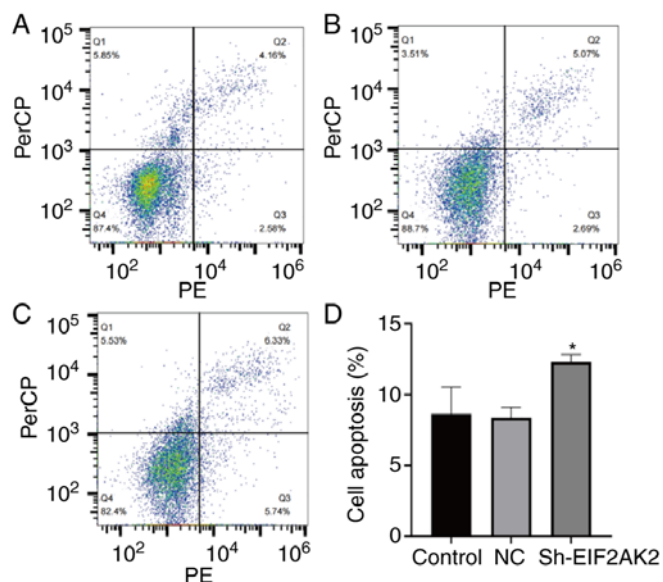


Figure 13. Analysis of PANC-1 cell apoptosis by flow cytometry. (A) Control (Normal PANC-1 cells). (B) NC (negative control). (C) sh-EIF2AK2. (D) sh-EIF2AK2 could promotes cell apoptosis. * $P < 0.05$ vs. Control and NC. EIF2AK2, eukaryotic translation initiation factor 2 α kinase 2; NC, negative control; si, small interfering; sh, short hairpin.

further confirmed the predictive role of EIF2AK2 expression in prognosis. These findings suggested that it could be a potentially valuable diagnostic and prognostic biomarker for pancreatic cancer.

Patients with pancreatic cancer have a poor prognosis, and the standard treatment combines surgery with chemotherapy and radiation therapy. During the past several years, immunotherapy has transformed the paradigm for cancer treatment, gaining recognition as a potential technique for treating certain malignancies (48). With the emergence of immunotherapy, several clinical studies have appeared to verify the efficacy of immunotherapy (49-51). These experiments explore the use of cellular transfer, immune checkpoint inhibitors (ICIs), cancer vaccines, and combinations of chemoradiotherapy and other molecular therapeutic approaches (52). Notably, due to their broad applicability across a broad spectrum of tumor types and excellent clinical response when treatment is successful, ICIs, a novel treatment approach comprised of anti-programmed cell death protein-1 (PD-1) and anti-programmed cell death protein ligand 1 (PD-L1) antibody treatments, have assumed the lead in the area of cancer immunotherapy (53,54). The majority of these experiments, however, have had uniformly poor outcomes. Pancreatic cancer is a tumor with low immunogenicity, which is attributable to a low tumor mutational burden. In light of this, it remains of the utmost importance to identify a potential biomarker of immune infiltration that may also predict the prognosis of a patient, as well as to determine potential molecular pathways that drive immunotherapeutic responses. In recent years, the incorporation of immunotherapy into the treatment of a number of solid tumors has led to a renaissance in oncology treatment (55).

Taking into account the potential oncogenic role of EIF2AK2 in pancreatic cancer, the present study assessed the relationship of EIF2AK2 with PD-1 (PDCD1), PD-L1

(CD274), PD-L2 (PDCD1LG2), CTLA4, LAG3, HAVCR2 and TIGIT. The use of monoclonal antibodies to inhibit CTLA4, PD-1 and PD-L1, thereby targeting immune checkpoint molecules, has led to a paradigm shift in the treatment of melanoma, lung, kidney, uroepithelial, head and neck cancer, and other malignancies (56). CTLA4 is an inhibitory receptor that regulates the initial phase of T-cell activation by competitively inhibiting the binding of B7 ligands to the costimulatory receptor CD28, preventing immune overactivation. PD-1 protein is another T-cell coinhibitory receptor with a more unique biological function than CTLA4; it binds PD-L1 and PD-L2 ligands, and blocks the activity of T-cell peripheral tissues. PD-L1 is the primary PD-1 ligand upregulated and detected in a variety of solid cancer types, including pancreatic, esophageal, gastric, colon, lung and breast cancer (57). A single phase II study, in which patients with locally advanced or metastatic pancreatic cancer were treated with ipilimumab monotherapy, revealed that of the 27 patients included, 74% had received prior gemcitabine-based chemotherapy (chemotherapy followed by immunotherapy can avoid damage to lymphocytes, improve immunity and enhance the advantages of chemotherapy and immunotherapy.). No responders were observed according to the assessment criteria, but a delayed response was reported in one subject whose initial progression was followed by regression of the primary tumor and metastases. The patient had significant new lesions in the mesentery of the small intestine after 9 months on Ipilimumab and eventually succumbed due to progression of liver metastases. The median OS was 4.5 months (58). Regarding PD-1/PD-L1 inhibitor monotherapy, Brahmer *et al* (59) tested the anti-PD-1 antibody BMS-936559 in a phase I trial involving 207 patients with different types of advanced cancer. Preliminary results from another randomized phase II trial were obtained from 65 patients with metastatic pancreatic cancer who had failed first-line 5-FU or gemcitabine therapy. Patients were randomized to receive durvalumab monotherapy or durvalumab in combination with tremelimumab. The median OS was 3.6 and 3.1 months, with disease control rates (60) (defined as stable disease + partial response + complete response) of 6 and 9%, respectively (59). Therefore, the relationship between EIF2AK2 and immune checkpoints was also assessed in the present study. In addition, antagonizing the CD155/TIGIT axis or LAG3 can induce profound antitumor responses as demonstrated by *in vitro* experiments (61,62). The aforementioned findings indicated that tumor immune escape may be involved in the EIF2AK2-mediated pancreatic cancer progression. In addition to monotherapy, combination therapy with immunosuppressants or with other antitumor agents is rapidly emerging. This phenomenon is due to the fact that single-agent checkpoint inhibitors have shown disappointingly limited activity in pancreatic cancer. The few studies of combination therapy have shown promise in terms of response (63-66). Patients with pancreatic cancer treated with checkpoint inhibitors have not shown improved response rates or OS. However, immunotherapy and its impact are topics of interest and possible ways to improve the prognosis of pancreatic cancer (67). This area of research includes both targeted therapies and antitumor vaccination.

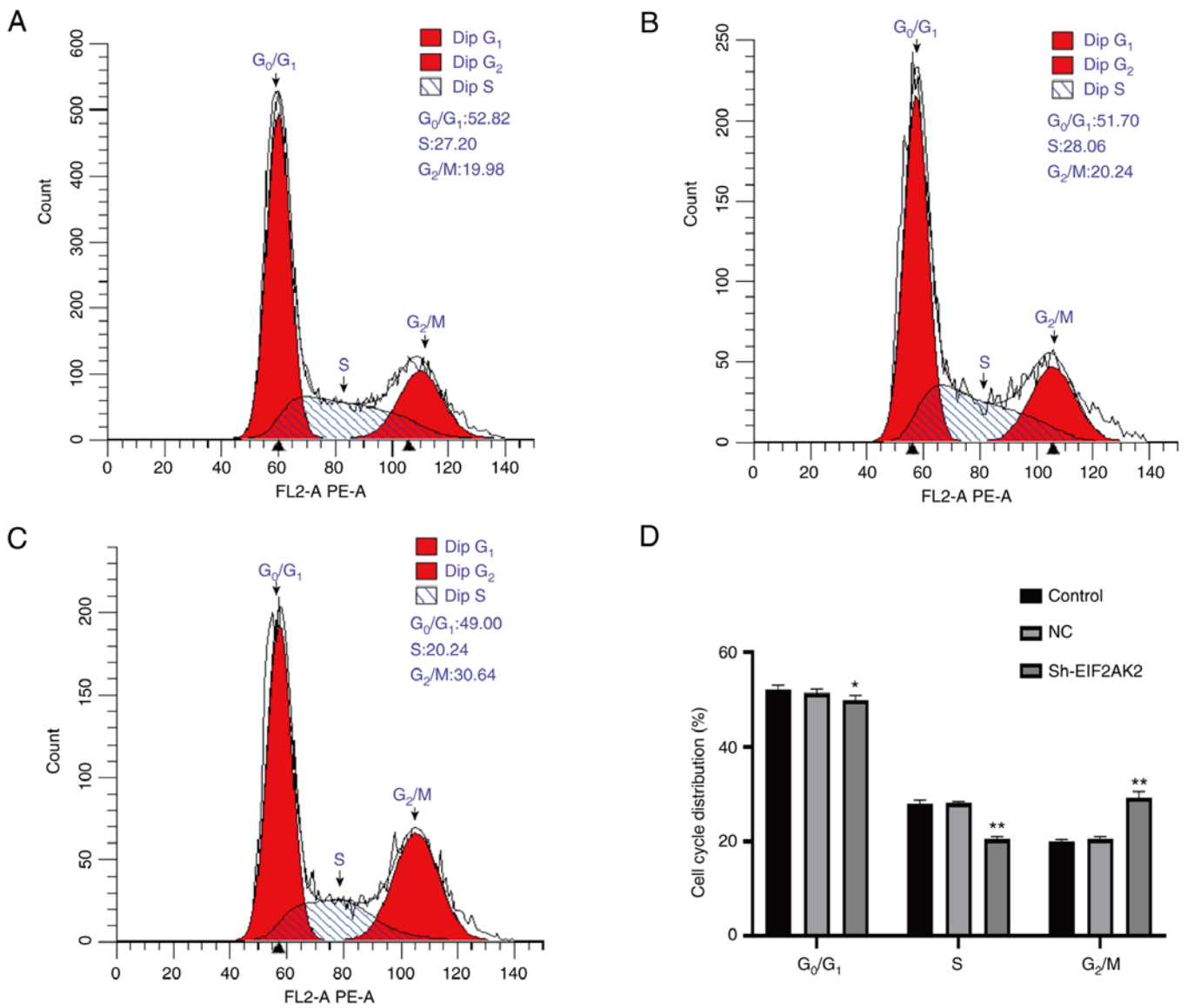


Figure 14. Analysis of PANC-1 cell cycle progression by flow cytometry. Cell cycle progression in the (A) control group, (B) NC group and (C) sh-EIF2AK2 group. (D) sh-EIF2AK2 could inhibit the cell cycle transition from G₁ to S phase, and induced cell cycle arrest in G₂/M phase. *P<0.05, **P<0.01 vs. Control and NC. NC, negative control; Sh, short hairpin.

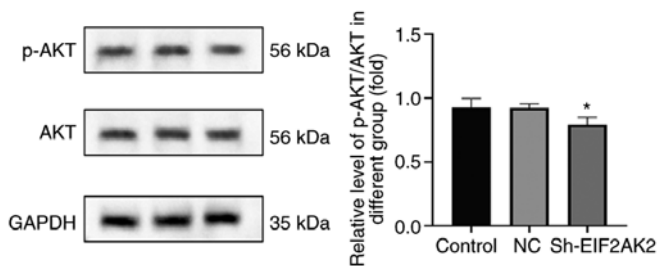


Figure 15. Effects of EIF2AK2 on the expression of AKT was detected by western blotting. *P<0.05 vs. Control and NC. EIF2AK2, eukaryotic translation initiation factor 2α kinase 2; NC, negative control; sh, short hairpin; p, phosphorylated.

Cancer-associated fibroblasts, tumor-infiltrating immune cells, endothelial cells and neurons are only a few of the nontumor components that comprise the tumor

microenvironment (68). Additionally, numerous extracellular matrix components play a vital role in the creation of an energetic TME with complex interactions between different internal components that promote tumor growth and treatment resistance (69). With the development of checkpoint inhibitor immunotherapy, tumor immunotherapy has evolved from an adjuvant therapy to an essential therapeutic strategy (70). The results of the present study indicated a link between EIF2AK2 expression and tumor-infiltrating immune cells in the TME. In addition, EIF2AK2 expression was associated with the StromalScore, ImmuneScore and the ESTIMATE score. EIF2AK2 was also revealed to be positively correlated with various immune cells, including aDCs, Th cells, Tem cells, Th1/Th2 cells, macrophages and pDCs. DCs are antigen-presenting cells that serve crucial roles in the establishment of adaptive and advanced immunity. aDCs can present antigens *in vivo* or *in vitro* by a variety of mechanisms, including an antibody-conjugated antigen

unique to aDCs and tumor-specific antigen capture. A substantial number of aDCs can travel to the region of the tumor and remain there for an extended period of time, hence augmenting the antitumor immune response (71,72). Since both Th1 and Th2 cells secrete cytokines to promote their own proliferation and inhibit the proliferation of the other, Th1 and Th2 cells are normally in a somewhat balanced state within the body (73). However, when the body has functional problems, the balance is frequently skewed to one side, a condition known as ‘Th1/Th2 drift’. Once the equilibrium between Th1 cells and Th2 cells is disrupted, the dynamic equilibrium of the human cytokine network is likely to be compromised, leading to the emergence and development of numerous illnesses (74).

Based on the analysis of the enrichment results, it can be concluded that knockdown of the EIF2AK2 gene reduces the proliferation and migration of PANC-1 cells, and can promote their apoptosis and inhibit the cell cycle. The experimental results that knockdown of EIF2AK2 promotes apoptosis in PANC-1 cells are clearly inconsistent with the findings reported above in the literature (36). Therefore it is necessary to review the basic principles of the EIF2AK2 pathway. When EIF2AK2 is activated, two representative downstream branches are stimulated: Pro-proliferative NF- κ B (pro-tumor effect) and pro-apoptotic eIF2 α (tumor suppressor effect). In addition to these two pathways, EIF2AK2 has several other downstream pathways, including PI3K, p38, p53 and PP2A (75). AKT, a PI3K downstream regulator, can phosphorylate target proteins through multiple downstream pathways and thus exert apoptosis-inhibiting effects (76). The present experimental results indicated that EIF2AK2 knockdown reduced p-AKT/AKT expression but increased apoptosis in PANC-1 cells. Therefore, whether EIF2AK2 has a biological function in promoting or inhibiting apoptosis in pancreatic tumor cells needs further investigation.

Unfortunately, there are some limitations in the present study. For example, the specific molecular pathway of EIF2AK2-mediated proliferation and migration remains to be elucidated. The function of EIF2AK2 *in vivo* is also not yet clear. We aim to conduct relevant *in vivo* studies in the future to address these deficiencies, such as colony formation, spheroid formation and tumorigenesis assays. However, the present study confirmed that EIF2AK2 is upregulated in pancreatic cancer and can effectively distinguish the degree of differentiation in patients with pancreatic cancer.

In conclusion, the present study demonstrated that EIF2AK2 may play a prognostic role and could be associated with immune infiltration in pancreatic cancer. As a direct consequence, EIF2AK2 has potential as a novel prognostic marker and as a prospective biomarker of new immunotherapeutic strategies.

Acknowledgements

Not applicable.

Funding

The present study was funded by the National Natural Science Foundation of China (grant no. 81960516).

Availability of data and materials

The datasets used and/or analyzed during the current study are available from the corresponding author on reasonable request.

Authors' contributions

HXD and KXZ conceived and designed the study and methodology. HXD, HW and HC performed biological experiments, data analysis, statistical work and manuscript preparation. HXD, ABD and XPM gathered clinical samples. KXZ and HXD confirmed the authenticity of all the raw data. All authors read and approved the final manuscript.

Ethics approval and consent to participate

All patients provided written informed consent and the present study was approved by the Ethics Committee of the First Hospital of Lanzhou University (Gansu, China; approval no. LDYYLL2023-304).

Patient consent for publication

Not applicable.

Competing interests

The authors declare that they have no competing interests.

References

- Mizrahi JD, Surana R, Valle JW and Shroff RT: Pancreatic cancer. *Lancet* 395: 2008-2020, 2020.
- Noë M, Hong SM, Wood LD, Thompson ED, Roberts NJ, Goggins MG, Klein AP, Eshleman JR, Kern SE and Hruban RH: Pancreatic cancer pathology viewed in the light of evolution. *Cancer Metastasis Rev* 40: 661-674, 2021.
- Cicenas J, Kvederaviciute K, Meskinyte I, Meskinyte-Kausiliene E, Skeberdyte A and Cicenas J: KRAS, TP53, CDKN2A, SMAD4, BRCA1, and BRCA2 Mutations in Pancreatic Cancer. *Cancers (Basel)* 9: 42, 2017.
- Mao X, Xu J, Wang W, Liang C, Hua J, Liu J, Zhang B, Meng Q, Yu X and Shi S: Crosstalk between cancer-associated fibroblasts and immune cells in the tumor microenvironment: New findings and future perspectives. *Mol Cancer* 20: 131, 2021.
- Wang M, Wu M, Liu X, Shao S, Huang J, Liu B and Liang T: Pyroptosis remodeling tumor microenvironment to enhance pancreatic cancer immunotherapy driven by membrane anchoring photosensitizer. *Adv Sci (Weinh)* 9: e2202914, 2022.
- Looi CK, Chung FF, Leong CO, Wong SF, Rosli R and Mai CW: Therapeutic challenges and current immunomodulatory strategies in targeting the immunosuppressive pancreatic tumor microenvironment. *J Exp Clin Cancer Res* 38: 162, 2022.
- Balachandran VP, Beatty GL and Dougan SK: Broadening the impact of immunotherapy to pancreatic cancer: Challenges and opportunities. *Gastroenterology* 156: 2056-2072, 2019.
- Li HB, Yang ZH and Guo QQ: Immune checkpoint inhibition for pancreatic ductal adenocarcinoma: Limitations and prospects: A systematic review. *Cell Commun Signal* 19: 117, 2021.
- Lou X, Gao D, Yang L, Wang Y and Hou Y: Endoplasmic reticulum stress mediates the myeloid-derived immune suppression associated with cancer and infectious disease. *J Transl Med* 21: 1, 2023.
- Smyth R and Sun J: Protein Kinase R in Bacterial Infections: Friend or Foe? *Front Immunol* 12: 702142, 2021.
- Meurs EF, Galabru J, Barber GN, Katze MG and Hovanessian AG: Tumor suppressor function of the interferon-induced double-stranded RNA-activated protein kinase. *Proc Natl Acad Sci USA* 90: 232-236, 1993.

12. Wu B, Song M, Dong Q, Xiang G, Li J, Ma X and Wei F: UBR5 promotes tumor immune evasion through enhancing IFN- γ -induced *PDL1* transcription in triple negative breast cancer. *Theranostics* 12: 5086-5102, 2022.
13. Shir A and Levitzki A: Inhibition of glioma growth by tumor-specific activation of double-stranded RNA-dependent protein kinase PKR. *Nat Biotechnol* 20: 895-900, 2002.
14. Yang X and Chan C: Repression of PKR mediates palmitate-induced apoptosis in HepG2 cells through regulation of Bcl-2. *Cell Res* 19: 469-486, 2009.
15. Minnee E and Faller WJ: Translation initiation and its relevance in colorectal cancer. *FEBS J* 288: 6635-6651, 2021.
16. Watanabe T, Ninomiya H, Saitou T, Takanezawa S, Yamamoto S, Imai Y, Yoshida O, Kawakami R, Hirooka M, Abe M, *et al*: Therapeutic effects of the PKR inhibitor C16 suppressing tumor proliferation and angiogenesis in hepatocellular carcinoma in vitro and in vivo. *Sci Rep* 10: 5133, 2020.
17. Kim SH, Forman AP, Mathews MB and Gunnery S: Human breast cancer cells contain elevated levels and activity of the protein kinase, PKR. *Oncogene* 19: 3086-3094, 2000.
18. Nakamura K, Aizawa K, Aung KH, Yamauchi J and Tanoue A: Zebularine upregulates expression of CYP genes through inhibition of DNMT1 and PKR in HepG2 cells. *Sci Rep* 7: 41093, 2017.
19. Zhang Y, Luo X, Lin J, Fu S, Feng P, Su H, He X, Liang X, Liu K and Deng W: Gelsolin promotes cancer progression by regulating epithelial-mesenchymal transition in hepatocellular carcinoma and correlates with a poor prognosis. *J Oncol* 2020: 1980368, 2020.
20. Watanabe T, Imamura T and Hiasa Y: Roles of protein kinase R in cancer: Potential as a therapeutic target. *Cancer Sci* 109: 919-925, 2018.
21. Song H, Tian D, Sun J, Mao X, Kong W, Xu D, Ji Y, Qiu B, Zhan M and Wang J: circFAM120B functions as a tumor suppressor in esophageal squamous cell carcinoma via the miR-661/PPM1L axis and the PKR/p38 MAPK/EMT pathway. *Cell Death Dis* 13: 361, 2022.
22. Vivian J, Rao AA, Nothaft FA, Ketchum C, Armstrong J, Novak A, Pfeil J, Narkizian J, Deran AD, Musselman-Brown A, *et al*: Toil enables reproducible, open source, big biomedical data analyses. *Nat Biotechnol* 35: 314-316, 2017.
23. Goldman MJ, Craft B, Hastie M, Repečka K, McDade F, Kamath A, Banerjee A, Luo Y, Rogers D, Brooks AN, *et al*: Visualizing and interpreting cancer genomics data via the Xena platform. *Nat Biotechnol* 38: 675-678, 2017.
24. Li K, Luo H, Luo H and Zhu X: Clinical and prognostic pan-cancer analysis of m6A RNA methylation regulators in four types of endocrine system tumors. *Aging (Albany NY)* 12: 23931-23944, 2020.
25. Barrett T, Wilhite SE, Ledoux P, Evangelista C, Kim IF, Tomashevsky M, Marshall KA, Phillippy KH, Sherman PM, Holko M, *et al*: NCBI GEO: Archive for functional genomics data sets-update. *Nucleic Acids Res* 41: D991-D995, 2013.
26. Barrett T, Trup DB, Wilhite SE, Ledoux P, Rudnev D, Evangelista C, Kim IF, Soboleva A, Tomashevsky M, Marshall KA, *et al*: NCBI GEO: Archive for high-throughput functional genomic data. *Nucleic Acids Res* 37: D885-D890, 2009.
27. Badaea L, Herlea V, Dima SO, Dumitrascu T and Popescu I: Combined gene expression analysis of whole-tissue and microdissected pancreatic ductal adenocarcinoma identifies genes specifically overexpressed in tumor epithelia. *Hepatogastroenterology* 55: 2016-2027, 2008.
28. Pei H, Li L, Fridley BL, Jenkins GD, Kalari KR, Lingle W, Petersen G, Lou Z and Wang L: FKBP51 affects cancer cell response to chemotherapy by negatively regulating Akt. *Cancer Cell* 16: 259-266, 2009.
29. Donahue TR, Tran LM, Hill R, Li Y, Kovichich A, Calvopina JH, Patel SG, Wu N, Hindoyan A, Farrell JJ, *et al*: Integrative survival-based molecular profiling of human pancreatic cancer. *Clin Cancer Res* 18: 1352-1363, 2012.
30. Janky R, Binda MM, Allemeersch J, Van den Broeck A, Govaere O, Swinnen JV, Roskams T, Aerts S and Topal B: Prognostic relevance of molecular subtypes and master regulators in pancreatic ductal adenocarcinoma. *BMC Cancer* 16: 632, 2016.
31. Nallagatla SR, Hwang J, Toroney R, Zheng X, Cameron CE and Bevilacqua PC: 5'-triphosphate-dependent activation of PKR by RNAs with short stem-loops. *Science* 318: 1455-1458, 2007.
32. Hu W, Zhou C, Jing Q, Li Y, Yang J, Yang C, Wang L, Hu J, Li H, Wang H, *et al*: FTH promotes the proliferation and renders the HCC cells specifically resist to ferroptosis by maintaining iron homeostasis. *Cancer Cell Int* 21: 709, 2021.
33. Livak KJ and Schmittgen TD: Analysis of relative gene expression data using real-time quantitative PCR and the 2(-Delta Delta C(T)) method. *Methods* 25: 402-408, 2001.
34. Yu G, Wang LG, Han Y and He QY: clusterProfiler: An R package for comparing biological themes among gene clusters. *OMICS* 16: 284-287, 2012.
35. Holcik M: Could the eIF2 α -independent translation be the achilles heel of cancer? *Front Oncol* 5: 264, 2015.
36. Karnam K, Sedmaki K, Sharma P, Venuganti VVK and Kulkarni OP: Selective inhibition of PKR by C16 accelerates diabetic wound healing by inhibiting NALP3 expression in mice. *Inflamm Res* 72: 221-236, 2023.
37. Lee YS, Kunkeaw N and Lee YS: Protein kinase R and its cellular regulators in cancer: An active player or a surveillant? *Wiley Interdiscip Rev RNA* 11: e1558, 2020.
38. Haines GK III, Panos RJ, Bak PM, Brown T, Zielinski M, Leyland J and Radosevich JA: Interferon-responsive protein kinase (p68) and proliferating cell nuclear antigen are inversely distributed in head and neck squamous cell carcinoma. *Tumour Biol* 19: 52-59, 1998.
39. Haines GK, Cajulis R, Hayden R, Duda R, Talamonti M and Radosevich JA: Expression of the double-stranded RNA-dependent protein kinase (p68) in human breast tissues. *Tumour Biol* 17: 5-12, 1996.
40. Shimada A, Shiota G, Miyata H, Kamahora T, Kawasaki H, Shiraki K, Hino S and Terada T: Aberrant expression of double-stranded RNA-dependent protein kinase in hepatocytes of chronic hepatitis and differentiated hepatocellular carcinoma. *Cancer Res* 58: 4434-4438, 1998.
41. Singh C, Haines GK, Talamonti MS and Radosevich JA: Expression of p68 in human colon cancer. *Tumour Biol* 16: 281-289, 1995.
42. Terada T, Ueyama J, Ukita Y and Ohta T: Protein expression of double-stranded RNA-activated protein kinase (PKR) in intrahepatic bile ducts in normal adult livers, fetal livers, primary biliary cirrhosis, hepatolithiasis and intrahepatic cholangiocarcinoma. *Liver* 20: 450-457, 2000.
43. He Y, Correa AM, Raso MG, Hofstetter WL, Fang B, Behrens C, Roth JA, Zhou Y, Yu L, Wistuba II, *et al*: The role of PKR/eIF2 α signaling pathway in prognosis of non-small cell lung cancer. *PLoS One* 6: e24855, 2011.
44. Kim SH, Gunnery S, Choe JK and Mathews MB: Neoplastic progression in melanoma and colon cancer is associated with increased expression and activity of the interferon-inducible protein kinase, PKR. *Oncogene* 21: 8741-8748, 2002.
45. Terada T, Maeta H, Endo K and Ohta T: Protein expression of double-stranded RNA-activated protein kinase in thyroid carcinomas: Correlations with histologic types, pathologic parameters, and Ki-67 labeling. *Hum Pathol* 31: 817-821, 2000.
46. Blalock WL, Grimaldi C, Fala F, Follo M, Horn S, Basecke J, Martinelli G, Cocco L and Martelli AM: PKR activity is required for acute leukemic cell maintenance and growth: A role for PKR-mediated phosphatase activity to regulate GSK-3 phosphorylation. *J Cell Physiol* 221: 232-241, 2009.
47. Roh MS, Kwak JY, Kim SJ, Lee HW, Kwon HC, Hwang TH, Choi PJ and Hong YS: Expression of double-stranded RNA-activated protein kinase in small-size peripheral adenocarcinoma of the lung. *Pathol Int* 55: 688-693, 2005.
48. Riley RS, June CH, Langer R and Mitchell MJ: Delivery technologies for cancer immunotherapy. *Nat Rev Drug Discov* 18: 175-196, 2019.
49. Immunotherapy shows promise in pancreatic cancer. *Cancer Discov* 9: 1330, 2019.
50. O'Hara MH, O'Reilly EM, Varadhachary G, Wolff RA, Wainberg ZA, Ko AH, Fisher G, Rahma O, Lyman JP, Cabanski CR, *et al*: CD40 agonistic monoclonal antibody APX005M (sotigalimab) and chemotherapy, with or without nivolumab, for the treatment of metastatic pancreatic adenocarcinoma: An open-label, multicentre, phase Ib study. *Lancet Oncol* 22: 118-131, 2021.
51. Rech AJ, Mick R, Martin S, Recio A, Aqui NA, Powell DJ Jr, Collignon TA, Trosko JA, Leinbach LI, Pletcher CH, *et al*: CD25 blockade depletes and selectively reprograms regulatory T cells in concert with immunotherapy in cancer patients. *Sci Transl Med* 4: 134ra62, 2012.
52. Reap EA, Suryadevara CM, Batich KA, Sanchez-Perez L, Archer GE, Schmittling RJ, Norberg PK, Herndon JE II, Healy P, Congdon KL, *et al*: Dendritic cells enhance polyfunctionality of adoptively transferred T cells that target cytomegalovirus in glioblastoma. *Cancer Res* 78: 256-264, 2018.

53. He X and Xu C: Immune checkpoint signaling and cancer immunotherapy. *Cell Res* 30: 660-669, 2020.
54. Bagchi S, Yuan R and Engleman EG: Immune Checkpoint Inhibitors for the Treatment of Cancer: Clinical Impact and Mechanisms of Response and Resistance. *Annu Rev Pathol* 16: 223-249, 2021.
55. Herzberg B, Campo MJ and Gainor JF: Immune checkpoint inhibitors in non-small cell lung cancer. *Oncologist* 22: 81-88, 2017.
56. Brower V: Checkpoint blockade immunotherapy for cancer comes of age. *J Natl Cancer Inst* 107: djv069, 2015.
57. Farasati Far B, Safaei M, Mokhtari F, Fallahi MS and Naimi-Jamal MR: Fundamental concepts of protein therapeutics and spacing in oncology: An updated comprehensive review. *Med Oncol* 40: 166, 2023.
58. Royal RE, Levy C, Turner K, Mathur A, Hughes M, Kammula US, Sherry RM, Topalian SL, Yang JC, Lowy I and Rosenberg SA: Phase 2 trial of single agent Ipilimumab (anti-CTLA-4) for locally advanced or metastatic pancreatic adenocarcinoma. *J Immunother* 33: 828-833, 2010.
59. Brahmer JR, Tykodi SS, Chow LQ, Hwu WJ, Topalian SL, Hwu P, Drake CG, Camacho LH, Kauh J, Odunsi K, *et al*: Safety and activity of anti-PD-L1 antibody in patients with advanced cancer. *N Engl J Med* 366: 2455-2465, 2012.
60. Brink GJ, Groeneweg JW, Hooft L, Zweemer RP and Witteveen PO: Response to systemic therapies in ovarian adult granulosa cell tumors: A literature review. *Cancers (Basel)* 14: 2998, 2022.
61. Gulhati P, Schalck A, Jiang S, Shang X, Wu CJ, Hou P, Ruiz SH, Soto LS, Parra E, Ying H, *et al*: Targeting T cell checkpoints 41BB and LAG3 and myeloid cell CXCR1/CXCR2 results in antitumor immunity and durable response in pancreatic cancer. *Nat Cancer* 4: 62-80, 2023.
62. Freed-Pastor WA, Lambert LJ, Ely ZA, Pattada NB, Bhutkar A, Eng G, Mercer KL, Garcia AP, Lin L, Rideout WM III, *et al*: The CD155/TIGIT axis promotes and maintains immune evasion in neoantigen-expressing pancreatic cancer. *Cancer Cell* 39: 1342-1360.e14, 2021.
63. Qian Y, Gong Y, Fan Z, Luo G, Huang Q, Deng S, Cheng H, Jin K, Ni Q, Yu X and Liu C: Molecular alterations and targeted therapy in pancreatic ductal adenocarcinoma. *J Hematol Oncol* 13: 130, 2020.
64. Conroy T, Castan F, Lopez A, Turpin A, Ben Abdelghani M, Wei AC, Mitry E, Biagi JJ, Evesque L, Artru P, *et al*: Five-Year outcomes of FOLFIRINOX vs gemcitabine as adjuvant therapy for pancreatic cancer: A randomized clinical trial. *JAMA Oncol* 8: 1571-1578, 2022.
65. Mahalingam D, Wilkinson GA, Eng KH, Fields P, Raber P, Moseley JL, Cheetham K, Coffey M, Nuovo G, Kalinski P, *et al*: Pembrolizumab in combination with the oncolytic virus pelareorep and chemotherapy in patients with advanced pancreatic adenocarcinoma: A phase Ib study. *Clin Cancer Res* 26: 71-81, 2020.
66. Conroy T, Hammel P, Hebbar M, Ben Abdelghani M, Wei AC, Raoul JL, Choné L, Francois E, Artru P, Biagi JJ, *et al*: FOLFIRINOX or gemcitabine as adjuvant therapy for pancreatic cancer. *N Engl J Med* 379: 2395-2406, 2018.
67. Schizas D, Charalampakis N, Kole C, Economopoulou P, Koustas E, Gkotsis E, Ziogas D, Psyrri A and Karamouzis MV: Immunotherapy for pancreatic cancer: A 2020 update. *Cancer Treat Rev* 86: 102016, 2020.
68. Hessmann E, Buchholz SM, Demir IE, Singh SK, Gress TM, Ellenrieder V and Neesse A: Microenvironmental determinants of pancreatic cancer. *Physiol Rev* 100: 1707-1751, 2020.
69. Neesse A, Bauer CA, Öhlund D, Lauth M, Buchholz M, Michl P, Tuveson DA and Gress TM: Stromal biology and therapy in pancreatic cancer: ready for clinical translation? *Gut* 68: 159-171, 2019.
70. Binnewies M, Roberts EW, Kersten K, Chan V, Fearon DF, Merad M, Coussens LM, Gabrilovich DI, Ostrand-Rosenberg S, Hedrick CC, *et al*: Understanding the tumor immune microenvironment (TIME) for effective therapy. *Nat Med* 24: 541-550, 2018.
71. Murphy TL and Murphy KM: Dendritic cells in cancer immunology. *Cell Mol Immunol* 19: 3-13, 2022.
72. Yin X, Chen S and Eisenbarth SC: Dendritic cell regulation of T helper cells. *Annu Rev Immunol* 39: 759-790, 2021.
73. Sanders VM: Epigenetic regulation of Th1 and Th2 cell development. *Brain Behav Immun* 20: 317-3124, 2006.
74. Dong C: Cytokine regulation and function in T cells. *Annu Rev Immunol* 39: 51-76, 2021.
75. Garcia-Ortega MB, Lopez GJ, Jimenez G, Garcia-Garcia JA, Conde V, Boulaiz H, Carrillo E, Perán M, Marchal JA and Garcia MA: Clinical and therapeutic potential of protein kinase PKR in cancer and metabolism. *Expert Rev Mol Med* 19: e9, 2017.
76. Fresno Vara JA, Casado E, de Castro J, Cejas P, Belda-Iniesta C and González-Barón M: PI3K/Akt signaling pathway and cancer. *Cancer Treat Rev* Apr 30: 193-204, 2004.



Copyright © 2023 Du et al. This work is licensed under a Creative Commons Attribution-NonCommercial-NoDerivatives 4.0 International (CC BY-NC-ND 4.0) License.